Student thesis series INES nr 414

Greenhouse gas flux at a temperate peatland: a comparison of the eddy covariance method and the flux-gradient method

Kristofer Karlsson

2017
Department of
Physical Geography and Ecosystem Science
Lund University
Sölvegatan 12
S-223 62 Lund
Sweden

Kristofer Karlsson (2017).
Greenhouse gas flux at a temperate peatland: a comparison of the eddy covariance method and the flux-gradient method
Master degree thesis, 30 credits in *Physical Geography*
Department of Physical Geography and Ecosystem Science, Lund University

Level: Master of Science (MSc)

Course duration: *November* 2015 until *January* 2017

Greenhouse gas flux at a temperate peatland: a comparison of the eddy covariance method and the flux-gradient method

---

Kristofer Karlsson

Master thesis, 30 credits, in
Atmospheric Science and Biogeochemical Cycles

Supervisors:

Magnus Lund
Department of Physical Geography and Ecosystem Analysis
Lund University

Patrik Vestin
Department of Physical Geography and Ecosystem Analysis
Lund University

Exam committee:

Janne Rinne
Department of Physical Geography and Ecosystem Analysis
Lund University

Lena Ström
Department of Physical Geography and Ecosystem Analysis
Lund University

Abstract

Northern peatlands have accumulated carbon for thousands of years and currently hold around one third of all soil carbon on earth. Large uncertainties are associated with predictions of how northern peatlands will react to climate change. This is because the cold, wet and anaerobic conditions lead to two opposing forces from a radiative forcing perspective – CO_2 sequestration from photosynthesis being greater than respiration, and release of the potent greenhouse gas CH_4. Accurately measuring fluxes of CO_2 and CH_4 is therefore key in order to understand the underlying processes and thereby implementing them in the global climate models.

In this thesis, the commonly used eddy covariance (EC) technique is compared to the less applied flux-gradient (FG) technique in order to assess the applicability of the use of CH_4 estimates by the FG method. The study took place at a temperate peatland in Southern Sweden, Fäjemyr, February-November 2015. CO_2 flux were estimated for each method and scalar similarity was assumed (with CO_2 as a reference) in order to estimate CH_4 flux using the FG method.

In general, there was good agreement between the CO_2 flux for both methods. Greatest agreement was found during daytime conditions with relatively high flux magnitudes (e.g. summer days) whereas worst agreement was found during nighttime and during periods of low flux magnitudes (e.g. winter and early spring). Since the agreement was satisfactory, the CH_4 flux by the FG method were deemed reliable. Furthermore, the CH_4 flux followed similar dependencies on temperature and water table depth as found for similar studies using other measurement techniques.

Cumulative CH_4 flux for the study period was estimated to 6.8 g C m^{-2}, which is middle of the range for similar sites, but also significantly higher than a previous study at Fäjemyr during a much drier year, indicating the importance of wetland hydrology on the carbon budget.

In conclusion, the FG technique is a good alternative to the EC method for northern peatlands and it is especially suitable for CH_4 measurements since the method is most reliable during the summer, when most CH_4 flux takes place.

Sammanfattning

Kol har lagrats is torvmarker i tusentals år och idag innehåller torvmarkerna ca en tredjedel av all markkol på jorden. Det råder stor osäkerhet hur torvmarker kommer att reagera på klimatförändringar. Detta beror på att de kalla, blöta och syrefattiga förhållandena leder till motsatta effekter för strålningsdrivningen; dels lagras CO_2 eftersom fotosyntesen är större än respirationen och dels släpper torvmarker ut den starka växthusgasen metan (CH_4). Därför är det viktigt att noggrant kunna mäta flöden av CO_2 och CH_4 för att förstå de underliggande processerna och därmed kunna implementera dem i globala klimatmodeller.

I denna studie jämförs den vanligare metoden eddy covariance (EC) med en mindre använd metod, flux-gradient (FG), för att utvärdera möjligheten att använda FG för att beräkna CH_4-flöden. Experimentet utfördes på en myr i södra Sverige, Fäjemyr, under februari-november 2015. Bägge metoderna användes för att beräkna CO_2-flöden, medan enbart FG-metoden användes för CH_4-beräkningar. Antagandet att transport av skalärer (t.ex. CO_2 och CH_4) sker likvärdigt genom turbulenta rörelser i atmosfären möjliggjorde sedan utvärdering av FG-metodens användningsbarhet för CH_4-mätningar.

Generellt sett överensstämde CO_2 -flödena väl mellan metoderna. Bäst överensstämmelse fanns under dagtid då flödena var höga (t.ex. sommardagar) och sämst överensstämmelse fanns under nätter och under perioder med låga flöden (t.ex. vinter och tidig vår). Eftersom överensstämmelsen var tillfredsställande ansågs CH_4-flödena från FG-metoden också vara pålitliga. Dessutom fanns förhållanden mellan CH_4-flöden och temperatur respektive grundvattennivån som andra studier också funnit med hjälp av andra mätmetoder.

Totala flöden av CH_4 under experimentet uppskattades till 6.8 g C m^{-2}. Jämfört med andra studier av CH_4-flöden från torvmarker placerar detta Fäjemyr i mitten av spannet. Å andra sidan är CH_4-flödet betydligt högre än en tidigare studie på Fäjemyr under ett extremt torrt år, vilket påvisar betydelsen av hydrologin för torvmarkers kolbudget.

Sammanfattningsvis är FG-metoden ett bra alternativ till EC-metoden för torvmarker och metoden är särskilt användbar för CH_4-mäningar eftersom mätningarna är mest pålitliga under sommaren då majoriteten av CH_4-flödena sker.

Table of Content

Introduction

Northern peatlands have accumulated carbon for thousands of years and hold almost one third of the total soil carbon pool (Post et al 1981). Since peatlands are characterized by waterlogged anaerobic conditions, methane (CH_4) is produced through methanogenesis and consequently leads to CH_4 release (Limpens et al., 2008). Although CH_4 is a very potent greenhouse gas, peatlands still act as net carbon sinks thanks to atmospheric CO_2 fixation by the vegetation outweighing decomposition (due to the anaerobic conditions).

As the northern regions are especially prone to extreme climate changes in the future (IPCC, 2013), it is uncertain what effects this will have on northern peatland carbon budgets (Lund et al., 2007; Lund et al., 2012). Due to the vast amounts of organic carbon stored in these soils, it is therefore essential to be able to accurately monitor and predict fluxes of carbon in northern peatlands.

The most commonly used technique to measure carbon fluxes in northern peatlands is the eddy covariance (EC) method. This micrometeorological technique utilizes high frequency measurements of both the vertical wind and a scalar, such as temperature or a greenhouse gas, in order to estimate flux (Foken et al., 2012). By using EC land-atmosphere exchange of greenhouse gases can be estimated on timescales ranging from hours to years without interfering on the environment (Moncrieff et al. 1997). Another advantage of this technique is that a single EC tower, consisting of a sonic anemometer and a fast-response gas analyzer on a mast, can cover large areas on ecosystem scales (Baldocchi 2003). Peatlands are especially suited for this method, since the underlying assumption is that the surrounding surface is flat and the vegetation composition is uniform (Baldocchi 2003), which is often fulfilled for this ecosystem type.

A less frequently used technique, the flux-gradient (FG) method, uses many of the same principles as EC, but does not require a fast-response gas analyzer. In this study, both methods are compared in order to assess the applicability of the FG technique for carbon flux estimates in northern peatlands.

1.1 Purpose and Study Aim

The main purpose of this thesis is to compare two greenhouse gas flux measurement techniques. In this study, the more common EC method is used for CO_2 and H_2O measurements, whereas a FG method is used to measure CH_4 flux in addition to CO_2 and H_2O flux.

The aim is to evaluate how the CO_2 flux measurements compare between the two techniques and from that analysis, using the scalar similarity theory, draw conclusions about the applicability of the FG CH_4 measurements. Since the main focus is to compare the two techniques, only the highest quality measurements will be kept for analysis, which means that more data is removed than for a traditional long-term carbon budget study.

Hypothesis:
The FG method will accurately capture the same physical transport processes of greenhouse gases as the eddy covariance technique, and can therefore be applied in order to estimate CH_4 flux as well as CO_2 flux.

Four study questions have been set up in order to test the hypothesis:

1. Does the gradient method capture the same diurnal and seasonal variability in CO_2 flux as the eddy covariance method?

2. How does the magnitude of CO_2 flux compare between the two methods?

3. During which meteorological conditions do the two methods perform similarly/differently?

4. Do the CH_4 fluxes seem reasonable compared to similar sites with various measurement techniques?

2. Background

2.1 Importance of northern peatlands

Northern peatlands are the most common type of wetland ecosystem, covering an area of $350 \cdot 10^6$ ha globally (Mitsch et al., 2009). From a biogeochemical cycle standpoint, northern peatlands are of high importance as about one third of all soil carbon (270-370 Tg C) is stored as peat (Gorham, 1991). The accumulation of peat in northern peatlands is not explained by remarkably high photosynthetic rates, but rather by the slow decomposition of plant litter caused by waterlogged, anoxic conditions. However, even though there is net sequestration of atmospheric CO_2, there is an opposing force to account for from a radiative forcing standpoint (Frolking et al., 2006). The anoxic conditions are favorable for CH_4 production by microbial activity (Limpens et al., 2008) and as a result, northern peatlands are sources of CH_4. Large uncertainties are associated with peatland contributions to climate modeling as there is a delicate balance between the cooling effect of CO_2 uptake and the warming effect of CH_4 release. Hydrology plays a major role in determining how northern peatlands will impact the climate in the future (Lafleur et al., 2003; Lund et al., 2012).

Peatland surfaces are rather uniform at an ecosystem scale compared to e.g. forests, but at a smaller scale they consist of a mosaic of wet hollows, dry hummocks, and intermediate zones (Laurila et al., 2012). One of the main methods of measuring land-atmosphere exchange is the chamber technique (Burba & Anderson, 2012), which is suited for small scale experiments. However, the limited spatial scale of chambers in combination with the fact that the chambers themselves interfere with the microclimate being studied, makes them less ideal for long-term and larger ecosystem scale studies. Peatland contribution of CO_2 flux are dominated by hummocks, whereas the contribution of CH_4 release is dominated by the wet hollows (Laurila et al., 2012). Therefore, measurements of peatlands would be most representative if covering areas of ecosystem scales.

2.2 Eddy Covariance Principles

The other main method to measure land-atmosphere gas flux is the micrometeorological method Eddy Covariance (EC), which is done by measuring the covariance between fluctuations in vertical wind speed and gas concentrations (e.g. CO_2). A typical EC setup consists of a sonic anemometer and a fast response (measurement rate 10-20 Hz) gas analyzer mounted on a mast or tower.

Air flow can be thought of as horizontal flow of small rotating air parcels, or eddies (Kaimal & Finnigan, 1994). Eddies vary in scale from kilometers to millimeters and transport energy and gases in the atmosphere (Foken, 2008). Although there is always a mix of eddy sizes, transport farther away from the ground are more frequently done by larger eddies, whereas smaller eddies dominate transfer closer to the ground (Burba & Anderson, 2012). The EC concept is valid in the inertial surface layer (the lower part of the planetary boundary layer), which is also called the constant flux layer. Within this layer, transport is dominated by turbulent processes and the vertical turbulent flux is assumed to be constant with height. Beneath the inertial surface layer, in the roughness sublayer (within and just above the canopy), flux is not constant with height (Foken, 2008). The inertial surface layer stretches from the top of

the roughness sublayer to a height that depends on atmospheric stability; from a few meters during stable conditions up to 100 m during unstable conditions (Foken, 2008).

Flux is defined as the amount of matter passing through a unit area per time. For CO_2, the flux unit commonly used is µmol m^{-2} s^{-1}. A positive value represents CO_2 release from land to the atmosphere, whereas a negative value represents CO_2 uptake from the atmosphere. EC flux can be calculated using equation 1.

$$F_x = \bar{\rho}_a \overline{w'C'} \qquad \text{(eq 1)}$$

Where F_x is the flux of gas x (e.g. CO_2), ρ_a is air density, w is vertical velocity, and C is the mixing ratio of the gas of interest. The overbar denotes time averaging and the primes denote fluctuations from the mean (Baldocchi, 2003).

The EC footprint, or source area, normally ranges between a few hectares to several square kilometers for horizontally homogeneous surfaces such as wetlands (Baldocchi, 2003). The size of the footprint depends on measurement height, surface roughness and thermal stability (Burba & Anderson, 2012). The higher the measurement height, the grater the footprint size. A general rule of thumb for EC studies is that during sufficiently turbulent conditions, the footprint distance, or fetch, is 100 times greater than the measurement height (Burba & Anderson, 2012). Surface roughness is commonly estimated as 0.15 · *canopy height* (Burba & Anderson, 2012). The fetch increases with decreased roughness. For peatlands, the roughness is low compared to e.g. forests (Burba & Anderson, 2012). Thermal stability affects the footprint size as well, as the fetch increases with increased stability (Leclerc, 1990). Daytime conditions, which are more unstable, therefore result in smaller footprints than stable nighttime conditions do.

2.3 Atmospheric Stability

Friction velocity, $u*$, is an important measure of atmospheric stability. It is calculated as:

$$u_* = \sqrt{-\overline{u'w'}} \qquad \text{(eq 2)}$$

where $u'w'$ is the covariance between the wind speed (m s^{-1}) in the horizontal (u) and vertical (w) direction (Tagesson, 2012).

Another measure of atmospheric stability is the stability parameter ζ:

$$\zeta = \frac{Z-d}{L} \qquad \text{(eq 3)}$$

where Z is the measurement height above ground, d is the displacement height (commonly estimated as $\frac{2}{3}$ of canopy height (Burba & Anderson, 2012)) and L is the Monin-Obukhov length, which is estimated by:

$$L = -\frac{u_*^3}{k\frac{g}{T}\frac{H}{\rho c_p}} \qquad \text{(eq 4)}$$

Where g is gravity (m s^{-2}), T is air temperature, H is sensible heat flux (W m^{-2}) and c_p is the specific heat of air at constant pressure (J kg^{-1} K^{-1}) (Tagesson, 2012).

2.4 Flux-Gradient Principles

The FG method is a combination of the EC method and a gradient method, and is suitable when a fast response gas analyzer is not available for the EC setup (Tagesson et al., 2012). In addition to the sonic anemometer used for the EC system, a FG setup also requires gas concentrations to be measured at different heights. By utilizing turbulence data (friction velocity and stability) collected by a sonic anemometer, in combination with gas concentrations gradients, the flux can be calculated using equation 5 (Denmead, 2008). This method has been used for both CO_2 and CH_4 flux studies before (e.g. Tagesson et al. 2012 and Sundqvist et al. 2015).

The FG method can be used to calculate gas flux using the following equation:

$$F_x = -K_c \frac{dC}{dZ} \qquad \text{(eq 5)}$$

Where F_x, the resulting flux of gas x, is a product of the turbulent diffusivity K_c and the concentration gradient $\frac{dC}{dZ}$.

Gradients $\frac{dC}{dZ}$ are obtained from dividing difference in gas concentrations with the height difference between concentration measurements.

$$\frac{dC}{dZ} = \frac{C_2 - C_1}{Z_2 - Z_1} \qquad \text{(eq 6)}$$

where C_1 and C_2 are concentrations at height Z_1 and Z_2 respectively.

Turbulent diffusivity K_c is calculated from friction velocity and stability provided by the EC measurements using the following equation (Tagesson, 2012):

$$K_c = \frac{k u_* (Z_2 - Z_1)}{\ln\left(\frac{Z_2}{Z_1}\right) - \psi_H(\zeta)_{Z_2} + \psi_H(\zeta)_{Z_1}} \qquad \text{(eq 7)}$$

Where k (0.4) is the von Kármán constant, u_* is the friction velocity, Z_2 and Z_1 are the upper and lower measurement heights respectively adjusted for displacement height. $\psi_H(\zeta)_{Z_2}$ is the diabatic correction function for heat profiles, which depends on stability *z/L* (Foken, 2008). The diabatic correction function of Högström (1988), originally derived by Businger and Dyer (Businger et al., 1971; Dyer 1974) is often used (e.g. Tagesson et al., 2012; Sundqvist et al., 2015).

The flux footprint for the FG method differs from that of the EC method, since the measurement heights are not the same for both methods. For neutral and unstable conditions, the measurement height for FG footprint purposes is defined as the geometric mean measurement height, $\sqrt{Z_1 Z_2}$. For stable conditions, the measurement height is defined as the arithmetic mean measurement height, $\frac{Z_1 - Z_1}{2}$ (Horst, 1999).

2.5 Study Background

The EC technique was first proposed in the mid 20th century, but was first applied for continuous studies of wetlands in the 1990's as a result of improvements in sonic anemometers and infrared gas analyzers (Foken et al., 2012). The first studies were carried out in North America, but soon also in Europe and Asia. One large motivator driving the expansion of EC measurements is the uncertainty of climate impacts of thawing permafrost regions, where the CO_2 and CH_4 balance is important (Laurila et al., 2012). Today there are hundreds of EC stations scattered globally, dozens of which are set up at northern peatlands. One of the sites, Fäjemyr, is the study site for this experiment. Greenhouse gas measurements have been performed at Fäjemyr since 2005 (Lund et al., 2007) – both using EC and chamber techniques.

3. Materials and Method

3.1 Site Description

The measurements for this study were performed at Fäjemyr (56º15'N, 13º33'E), which is a natural peatland located 25 km northwest of Hässleholm in southern Sweden. Fäjemyr is located in the temperate climate zone and the altitude is 140 m above sea level. Than mean annual temperature is 6.2 ºC, with monthly averages ranging from a minimum of -2.4 ºC in January to a high of 15.1 ºC in July. The annual precipitation is 700 mm (Lund, 2009). Long-term temperature and precipitation averages were recorded at nearby SMHI weather stations (temperature: Markaryd, precipitation: Hässleholm).

A 4-6 m layer of peat separates the underlying bedrock from the ground surface, with the deepest layer dated to about 6500 years old (Lund et al., 2007). Small hummocks, lawns and hollows make out the peatland surface topography, with hummocks being most frequent due to relatively dry conditions (Lund, 2009).

Besides some scattered small trees (*Pinus sylvestris and Betula pubescens*), the vegetation is dominated by dwarf shrubs such as *Calluna vulgaris* and *Erica tetralix*, sedges (Eriophorum vaginatum) and *Sphagnum* mosses (Lund et al., 2009).

As seen in Figure 1 (b), the EC mast is set up in the southern part of Fäjemyr, with at least 290 m of homogeneous surface properties surrounding in all directions (Lund et al., 2007).

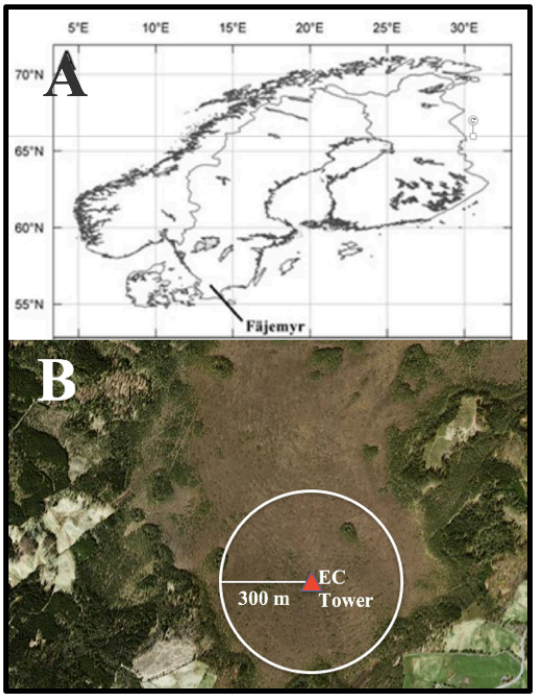

Figure 1: Map of Scandinavia pinpointing Fäjemyr (a) (Lund et al., 2007) and an aerial photograph over Fäjemyr (Eniro, 2016). The red triangle indicates the location of the EC tower. The bog extends nearly 300 m in all directions around the EC tower.

3.2 Measurement Setup

During the fall of 2013, a new EC tower was built in order to replace an older EC setup. In February 2015, a FG system was added to the EC setup (sharing the sonic anemometer), adding CH_4 measurements in addition to CO_2 and H_2O measurements. The two systems, using EC and FG techniques, ran simultaneously from February 12 2015 to November 5 2015, measuring CO_2 and H_2O (EC system) and CO_2, H_2O and CH_4 (FG system).

3.2.1 EC Setup

The EC tower seen in Figure 2 (a) consisted of a three-dimensional sonic anemometer (Gill HS-50, Gill Instruments Inc., UK) and an enclosed path infrared gas analyzer (LI-7200, Li-Cor Inc, USA) measuring CO_2 and H_2O concentrations. The anemometer (Figure 2 (b)) and gas analyzer were mounted on a mast 3 m above ground. Air was sucked from the same height as the center of the sonic anemometer (10 cm horizontal separation, see Figure 2) and transported through a 1 m tube (5 mm inner diameter) at a flowrate of 15 l min^{-1}, finally passing through the LI-7200 (also 15 l min^{-1} flowrate). In order to avoid condensation in the tube caused by underpressurization, the pump was placed after the LI-7200. An LI-7550 logger was installed at the base of the mast to record sonic anemometer and gas measurements at a frequency of 20 Hz and saved data as 30-minute log files.

The canopy height was estimated to be 0.30 m throughout the study period and there was never significant snow to affect the canopy height or the height of the sonic anemometer. Displacement height and roughness length were set to 0.67 · *canopy height* and 0.15 · *canopy height* respectively in the flux calculation software.

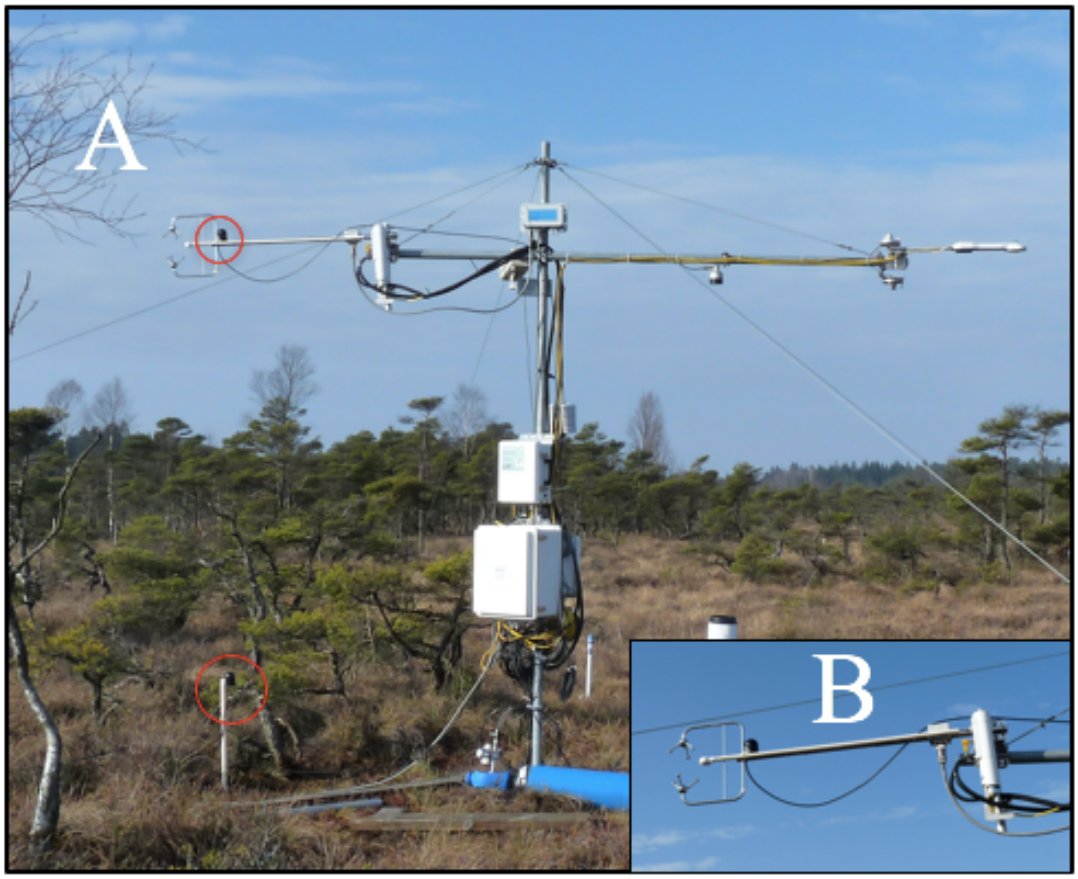

Figure 2: The EC mast with instrument setup (a) and close-up view of the sonic anemometer and gas analyzer (b). Red circles indicate upper and lower intake levels for the FG system.

3.2.2 FG Method Setup

The experimental setup for the FG method followed the method of a previous study where the FG technique was used for CH_4 flux measurements (Tagesson et al., 2012). A Fast laser off-axis ICOS (integrated cavity output spectroscopy) analyzer (GGA, Los Gatos Research, USA) measured CO_2, H_2O and CH_4 concentrations at two heights (3.00 m and 0.55 m above ground) on the existing EC tower at a rate of 1 Hz. The gas analyzer was located in a small hut approximately 20 m from the EC tower. Air was continuously sucked from each height through tubes (length: 20 m, inner diameter: 4 mm) at a flow rate of 5 L/min using independent membrane pumps located in the hut. Before the air entered the analyzer, the air was mixed in independent 4 L mixing volumes (Figure 3). Air was continually sucked from both heights and passed through separate mixing volumes. A magnetic valve directed the air flow from the different intake heights through the gas analyzer, alternating between heights every five minutes. Excess airflow was ventilated through a T-connector. Subsamples of air from the mixing volumes entered the gas analyzer at a flow rate of 0.4 l min^{-1}.

Gas concentrations were recorded at a rate of 1 Hz and alternated between the two levels every 5 minutes. Hourly output files were generated with the gas concentrations of CH_4, CO_2 and H_2O.

Figure 3: The inside of the small hut located close to the EC tower. Mixing volumes are visible in the top of the photo and the gas analyzer (LGR) in the bottom left corner.

3.2.3 Additional environmental measurements

In addition to the two flux measurement setups, other meteorological and environmental variables were recorded and saved as 30-minute averages to a CR1000 data logger (Campbell Sci., USA) using the instruments specified in table 1.

Table 1: Environmental measurements and corresponding instrument used in addition to the EC and FG setup.

Name	**Description**	**Instrument/Manufacturer**
Air T	Air Temperature (C)	CS215, Campbell Sci.
Soil T 5cm	Soil Temperature 5 cm in representative area (C)	P107 Probe, Campbell Sci.
Soil T 20 cm	Soil Temperature 5 cm in representative area (C)	P107 Probe, Campbell Sci.
RH	Relative Humidity (%)	CS215, Campbell Sci.
Precipitation	Precipitation (mm)	52203, RM Young tipping bucket rain gauge
WTD	Water table depth (relative to peat layer)	Pressure transducer, CS451, Campbell Sci.
P	Atmospheric pressure (mbar)	Setra 278, Campbell Sci
PAR	Incoming photosynthetic active radiation (µmol m^{-2} s^{-1})	SKP 215, Skye Instruments

3.3 Data analysis - EC Calculations

Flux calculations for the EC system were done using the computer software EddyPro version 6.0.0 (LI-COR Inc., Nebraska, USA). EddyPro processed the 20 Hz raw data and calculated 30-minute average values and statistics from data provided by the sonic anemometer and LI-7200 gas analyzer measurements. Statistical tests for the 20 Hz raw data are based on Vickers and Mahrt (1997) and included:

- **Spike count/removal test**
  - Despiking procedure which detects and removes short-termed outliers in the data series.

- **Amplitude resolution test**
  - Detects periods where fluctuations cannot be captured accurately due to insufficient amplitude resolution (due to e.g. weak winds and stable conditions or faulty instrument).

- **Drop-out test**
  - Detects relatively short periods during which the time series sticks to some value that is statistically different from the average value over the whole period

- **Absolute limit test**
  - Detects for each variable if at least one value during each time series is outside of a plausible range. The test is performed after despiking (i.e. outranged values are not spikes and can therefore affect fluxes unless they are removed).

- **Discontinuity test**
  - Detects semi-permanent changes (as opposed to sharp changes associated with smaller scale fluctuations) caused by discontinuities.

Default hard flag values for accepted ranges and thresholds were used for all statistical tests. High frequency spectral corrections followed Fratini et al. (2012), which minimizes the effect of relative humidity on water vapor in the sampling line (LI-COR, 2016). The method by Fratini et al. (2012) was tested with an identical enclosed-path gas analyzer (LI-7200) as for this study and was therefore picked over the older EddyPro default (Moncrieff et al., 1997).

3.3.1 Micrometeorological Test

Both the EC and the FG method require that the state of micrometeorological variables are steady and that there is sufficient atmospheric mixing. Therefore, data was filtered following the steady state test and the integral turbulence test (Foken, 2008). The 0-1-2 flagging policy developed by Mauder and Foken (2004) was used in EddyPro to assess the quality of the data:

0 – Highest quality data, use in fundamental research possible
1 – Good quality data, no restrictions for use in long term observation programs
2 – Questionable data quality, gap filling necessary

As the primary objective of this study is to compare the two methods rather than calculating annual budgets, the strictest quality class of 0 was used even though this resulted in a greater data loss.

3.3.2 Signal Strength

The LI-7200 average signal strength is a measure that can be used to assess how clean the instrument window/mirrors are, and hence a measure of how reliable the concentration measurements used for flux calculations are. As the instrument becomes dirtier, the signal strength decreases. Values range between 0-100, where a value of 100 is clean, 80 is relatively dirty, 50 is very dirty, and 0 meaning that there is no signal at all (LI-COR, 2016). The best practice is therefore to clean the instrument on a regular basis in order to obtain the most reliable results. Throughout the study period, the instrument was cleaned the following five times in order to increased signal strength:

- February 2
- April 16
- August 12
- August 24
- October 16

The long gap between April 16 and August 12 proved to be costly due to declining signal strength throughout the summer leading up to August 12. Figure 4 shows the measured CO_2 concentration (a), signal strength (b), and daily standard deviation for the signal strength (c). Dates of instrument cleaning are marked with dashed lines. CO_2 concentrations are expected to decrease slightly during northern hemisphere summer due to photosynthesis. However, in this study, summer concentrations were significantly lower than expected values, reaching levels between 300-350 ppm June-August. The signal strength drifts (decreases) after each cleaning, which could be manageable to a certain extent had it not been for the increasing signal strength diurnal variation during the summer (P Vestin & M Mölder 2016, personal communication, November). The standard deviation clearly indicates the significantly increased diurnal variation during the summer leading up to August 12. Figure 5 shows a closer look at the signal strength before and after cleaning. Pre-cleaning, the signal strength is low and varies greatly between day and night. Immediately following cleaning on August 12 (dashed line in Figure 5), the signal strength returns to a higher value and the diurnal variability is negligible. Figure 6 shows the CO_2 concentration scattered vs. signal strength. The CO_2 concentration appears to decrease as the signal strength decreases, especially below signal strength of 55 (red dashed line).

Based on the analysis of CO_2 concentration, signal strength and resulting fluxes (presented in results), two signal strength criteria were set up in order to ascertain that only the top-quality data be accepted for method comparison purposes:

$$\text{30-minute signal strength} \geq 55 \ \& \ \text{daily standard deviation} \leq 2$$

These thresholds were carefully chosen in order to both maintain the high-quality data but at the same time keeping as much data as possible. Figure 4 illustrates that most of the summer data is removed due to low quality signal strength.

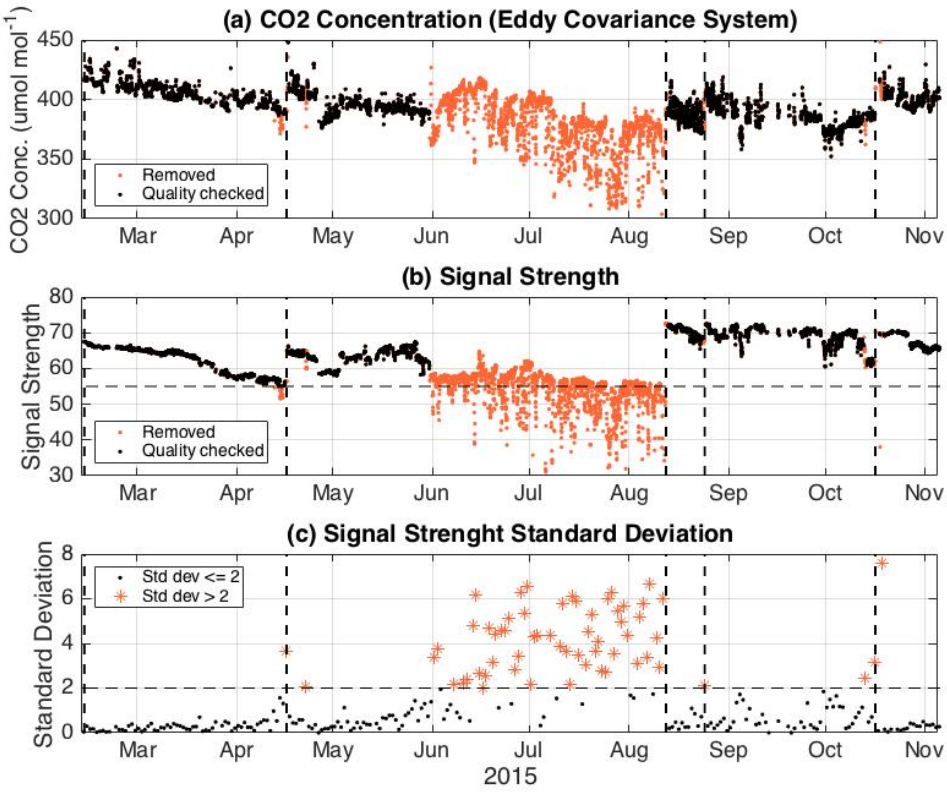

Figure 4: 30-minute CO_2 concentration (a), 30-minute signal strength (b) and daily signal strength standard deviation (c) for the study period. The horizontal dashed lines in (b) and (c) mark the acceptance level for signal strength (55) and signal strength standard deviation (std dev > 2), respectively. Red colors indicate removed data due to low quality signal strength and the vertical dashed lines indicates LI-7200 cleaning dates.

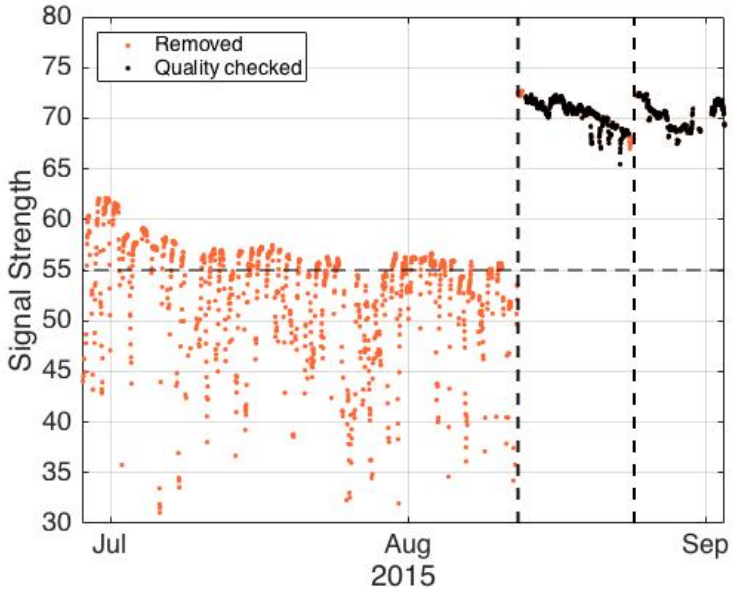

Figure 5: 30-minute signal strength values before (red) and after (black) cleaning the LI-7200 on August 12 cleaning, marked by the dashed line.

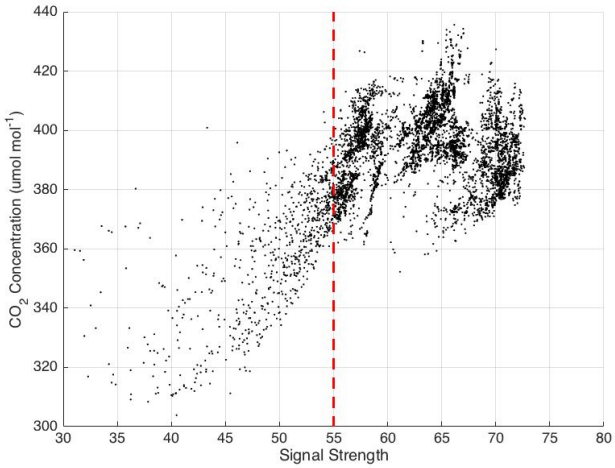

Figure 6: 30-minute CO_2 concentration scattered vs. signal strength. The dashed line indicates signal strength = 55.

3.3.3 *u** filtering

Loss of usable data due to nighttime stability is one of the drawbacks of the EC technique (Baldocchi, 2003). Low values of friction velocity, u^*, is one measure to identify insufficient atmospheric mixing often found during nighttime. Lund et al. (2007) found that there was a positive relationship between nighttime CO_2 flux and u^* for conditions where $u^* < 0.1$ at Fäjemyr. Therefore, the same threshold value was used for this study and as a result, 13.1 % of the data set was removed. Worth noting is that much of the removed data due to low u^* is also removed by Foken's micrometeorological tests.

3.4 Data analysis – FG Calculations

All data processing for the FG system was performed in MATLAB (version R2015b), by modifying a series of scripts originally created by Patrik Vestin.

3.4.1 Concentration gradient calculations

Since EddyPro generates EC gas fluxes as half hourly averages, the same time interval was used for the FG system. Each 1-hour log file with raw data consisted of 12 five-minute measurements (of 1 Hz) as the intake alternated between the upper and lower level every five minutes. A typical hour of CH_4 concentration raw data is depicted in Figure 7, where the alternating levels are clearly evident due to shifts in concentrations. The upper level has lower concentrations than the lower level, indicating an upwards directed flux.

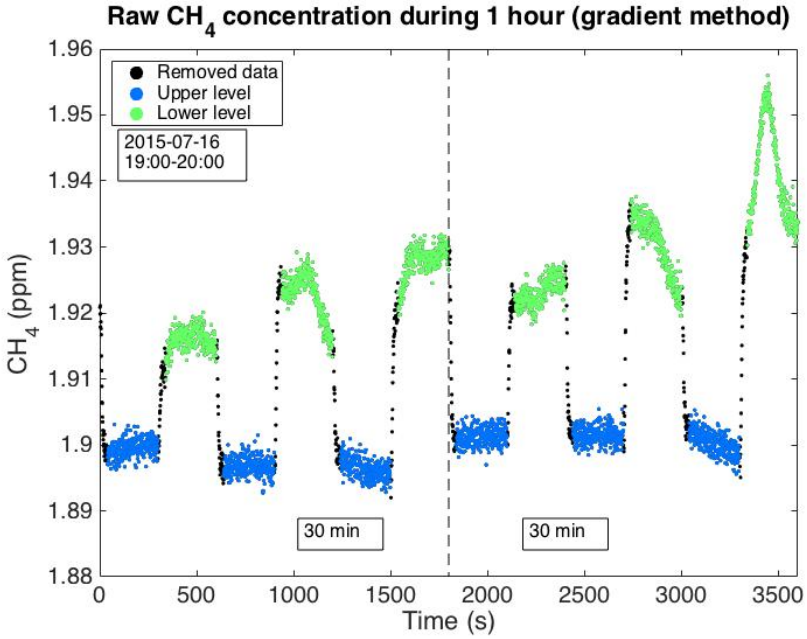

Figure 7: Typical 1-hour time series of CH_4 concentration measurements alternating between the upper level (blue) and the lower (green). Black dots were removed before averages were calculated. The principle is the same for CO_2 measurements.

Concentration difference between heights, *dC*, for each 30-minute period was calculated using the average concentration of each level per half hour, excluding the first 40 seconds of each five-minute period as there is a lag between the time the switch is made and the time at which a new steady concentration is obtained. This lag is a result of the time needed for air to be replaced in the analyzer cell and in the tubes after the T-connector. For each level and half hour, 780 records (3 · 260 seconds) therefore remained to be averaged for concentration gradient calculations.

Concentration data outside of a plausible range (defined below) were excluded from the 30-minute averaging used for concentration gradient calculations:

CO_2: 350 ppm – 800 ppm
CH_4: 1.5 ppm – 4.0 ppm
H_2O: 0 ppm – 30000 ppm

For each 5-minute period at each level, spikes were removed following Schmid et al. (2000), which is an iterative process in which values are removed if they differ by more than a discrimination factor times the standard deviation of the average interval. Spikes were removed in 6 iterations, using discrimination factors of 3.5, 3.8, 4.1, 4.3, 4.7, and finally 5.0. For each iteration, the standard deviation decreases as spikes are removed. Once the spikes were removed, 30-minute averages were calculated from the three 5-minute periods (minus the first 40 seconds) for each level respectively.

Concentration averages were dilution corrected for water vapor by converting the measured mole fractions to mixing ratios. This is important since the gradients in H_2O can be much larger than the gradients in CO_2 or CH_4. First, H_2O concentration was corrected for water vapor by converting the measured mole fraction to mixing ratio.

The H_2O mixing ratio was then used to correct the CO_2 concentrations. Finally, CH_4 concentrations were corrected for both corrected water vapor and for corrected CO_2. Although the CO_2 effect on CH_4 concentration is very small, it is conceptually correct to do this correction (P Vestin 2016, personal communication, December).

Before the concentration gradients were calculated, the concentration units were first converted from µmol mol^{-1} to µmol m^{-3} by using the ideal gas law.

$$pV = nRT \qquad \text{(eq 8)}$$

Where p is pressure (Pa), V is volume (m^3), n is number of moles, R is the universal gas constant ($m^3PaK^{-1}mol^{-1}$) and T is temperature (K). Since the desired units were µmol m^{-3}, the measured concentrations (µmol mol^{-1}) were multiplied by a conversion factor $\frac{p}{RT}$ (mol m^{-3}).

Pressure and temperature for the unit conversion were obtained from the Setra 278 barometer and the CS215 thermometer respectively.

Finally, the 30-minute concentration gradients $\frac{dC}{dZ}$ and corresponding standard deviations were calculated.

3.4.2 Turbulent Diffusivity calculations

Turbulent diffusivity is calculated by eq 7, where friction velocity and stability are provided by the EC measurements. The diabetic correction function for heat, which depends on stability z/L, is taken from Högström (1998) and is also used by e.g. Tagesson et al. (2012) and Sundqvist et al. (2015).

3.4.3 Method for estimating error in fluxes (FG method)

The total error in fluxes, $Flux\_Err\_Tot$, is a combination of error in concentration gradients and the error in turbulent diffusivity. Propagation of errors says that the measurements should have noise added in quadrature.

$$Flux\_Err\_Tot = \sqrt{Flux\_Err\_Grad^{\,2} + Flux\_Err\_K^{2}} \qquad \text{(eq 9)}$$

Where $Flux\_Err\_Grad$ is the flux error caused by errors in concentration gradients and $Flux\_Err\_K$ is the flux error caused by errors in turbulent diffusivity.

$Flux\_Err\_K$ is estimated by multiplying the concentration gradient ($\frac{dC}{dZ}$) by the error in turbulent diffusivity (Err_K), which was estimated to be 0.02 for $u^* > 0.06$ ms^{-1}. As no error estimate of turbulent diffusivity was made specifically for this study, the value from another study (using a different sonic anemometer) was used (P Vestin, unpublished results). Data was removed when $u^* < 0.06$ ms^{-1} as the error in diffusivity has been found to no longer be constant below this value (P Vestin, unpublished results).

$$Flux\_Err\_K = \frac{dC}{dZ} Err\_K \qquad \text{(eq 10)}$$

$Flux\_Err\_Grad$ is calculated by multiplying the error in diffusivity by the error in gradient (Err_X) divided by difference in height between the intake tubes ($DeltaZ$ = 3.00 m - 0.55 m = 2.45 m).

$$Flux\_Err\_Grad = K \frac{Err\_X}{DeltaZ} \qquad \text{(eq 11)}$$

Err_X is the error in CH_4 and CO_2, which is given by quadratic summation of the precision of the LGR.

The precision for each gas was obtained from the LGR manual for 100 seconds (1 standard deviation). The precision for each gas was:

- CH_4: 0.25 ppb
- CO_2: 40 ppb

Since the time-period used for the gradients was 780 seconds (at 1 Hz sampling frequency) per level and not 100 seconds, the actual precision may have been better. However, the above values were still used in order to maintain a strict quality assessment throughout the study.

Only values with total flux errors < 40 µmol m^{-2} hr^{-1} (CH_4) and <1 µmol m^{-2} s^{-1} (CO_2) were kept for further analysis. The limits used for acceptance were determined through visual interpretation of the error distribution for each gas respectively.

3.5 u^* filtering distinction between methods

An important distinction is made for filtering for low u^* between the two methods. For EC, data was removed for low u^* situations, defined as $u^* < 0.1$ m s^{-1}, because the assumption that the vertical turbulent flux dominating over e.g. vertical advection and storage change is not valid for such low turbulence. For FG on the other hand, fluxes collected during conditions with $u^* < 0.06$ m s^{-1} were removed since the error in diffusivity was not assumed to be constant below this value. For direct method comparison, all fluxes collected during conditions with $u^* < 0.1$ m s^{-1} have consequently been removed (as a combination of the final quality tests are used). However, for FG gap-filled CO_2 time series and for CH_4 purposes, only fluxes collected during conditions with $u^* < 0.06$ ms^{-1} were removed.

3.6 EC Flux Footprint

For EC, EddyPro automatically calculates distances of cumulative contributions for each 30-minute flux for different cumulative contribution percentages (e.g. 70 % and 90 % cumulative contribution), which gives a good indication of whether the measured flux originated from the intended footprint area. The 90 % cumulative percentage distances were of analyzed in order to make sure that the footprint did not extend beyond the homogeneous peatland area of Fäjemyr.

3.7 Gap Filling

Micrometeorological tests, statistical tests, and error estimations all removed data, resulting in non-continuous 30-minute CO_2 flux time series for the study period. In order to estimate the cumulative flux, all gaps had to be filled. Gaps in CO_2 flux were filled using a MATLAB script by Magnus Lund (last modified 2015) based on Reichstein et al. (2005), which estimates CO_2 flux for each 30-minute gap based on CO_2 flux (only quality checked) for similar meteorological conditions. The input variables were air temperature, photosynthetic active radiation (PAR) and vapor pressure deficit (VPD), which were all measured at the EC mast. An initial window size of ± 5 days was used in order to find similar meteorological conditions for gaps in CO_2 flux. The acceptable range for air temperature, PAR, and VPD were 2.5 degrees C, 20 μmol m^{-2} s^{-1}, and 0.5 kPa respectively. The window was expanded to ± 10 days if no conditions were satisfactory within the original window. If the conditions are not fulfilled within the larger window either, only the PAR requirement is used - first for the smaller window, and if needed, the larger window is used. Finally, if no conditions match the PAR requirements, mean diurnal variation is used for the initial window, or if needed, the larger window. This is done by averaging all valid CO_2 flux within the appropriate window (at least 4 valid values are required).

The few remaining 30-minute gaps after the first gap-fill run (EC: 90, FG: 41) were filled by repeating the same methodology, only using the gap-filled CO_2 flux as input the second time around (instead of only quality tested CO_2 flux). After the second gap-filling run, all gaps were successfully filled. The second run did not alter the average CO_2 flux, but the cumulative sums were changed to slightly more representative values as all remaining gaps were daytime values with negative flux (CO_2 uptake).

The long summertime gap in EC CO_2 flux resulting from low quality signal strength was gap filled using the FG CO_2 flux. This was the only way to realistically fill such a large gap.

The same gap-filling methodology does not apply to CH_4 flux as the underlying physical processes for CO_2 flux (i.e. photosynthesis and respiration) do not apply for CH_4 flux. Sine there is little diurnal variation in CH_4 flux, daily average CH_4 flux was instead calculated before linear interpolation was used to fill the few daily gaps that remained. The requirements for daily values to be calculated were that at least 12 (out of 48) 30-minute values passed all quality tests, and that they were within 5 standard deviations from the daily mean. Linear interpolation is a simplified method compared to many advanced methods such as multiple linear regression or neutral networks (Dengel et al., 2013). However, linear interpolation is sufficient for the purpose of this study.

4. Results and Discussion

Between February 12, 2015 and November 5, 2015, the two systems operated simultaneously, providing the opportunity to compare and assess the two methods to each other. The collected data was continuous and only consisted of shorter breaks in data. However, after quality assessment of micrometeorological conditions, instrument reliability, error estimation etc., much of the original 30-minute data was removed.

The results of the quality tests will first be presented, followed by meteorological conditions and CO_2 concentrations. Thereafter the CO_2 flux and comparison between the two methods will be presented and analyzed. Finally, the CH_4 results are presented and the applicability of the FG method is discussed.

4.1 Quality control

The effect of each individual quality test on EC and FG are presented in Table 2. Most of the removed data due to the micrometeorological tests (steady state, integral turbulence, and u^*) were due to stable nighttime conditions, which is common for EC measurements (Foken et al., 2012). Again, the strictest quality criteria were chosen for the steady state and integral turbulence test, which removed some data normally accepted for long-term ecosystem studies.

The statistical tests performed in EddyPro removed more EC data than FG data since only the sonic anemometer data was tested for FG purposes, whereas both the sonic anemometer and the gas analyzer data was tested for EC.

Table 2: Percent of 30-minute data remaining for EC (left) and FG (right) after each individual quality test. The combined result of all applied tests is listed as Final CO_2 and Final CH_4.

Quality Test	EC Remaining
Steady state & integral turb. (H)	80 %
Steady state & integral turb. (CO_2)	63 %
u^* (EC)	87 %
Spikes	77 %
Amplitude Resolution	93 %
Drop Outs	96 %
Absolute Limits	91 %
Discontinuities	89 %
Signal Strength	59 %
Final CO_2	**29 %**

Quality Test	FG Remaining
Steady state & integral turb. (H)	80 %
u^* (FG)	92 %
Spikes	91 %
Amplitude Resolution	97 %
Drop Outs	100 %
Absolute Limits	95 %
Discontinuities	90 %
Flux Error CO_2	76 %
Flux Error CH_4	79 %
Final CO_2	**58 %**
Final CH_4	**55 %**

The test that removed most EC data was the signal strength evaluation (59 % remained). Almost all the lost data due to bad signal strengths of the LI-7200 occurred during June, July and early August, which limits the available data for method comparison.

Although heavy rain is known to cause inaccurate readings for both the sonic anemometer and the gas analyzer (Burba & Anderson, 2012) rain periods were not explicitly removed since other quality tests also removed the same data. 80 % of the 30-minute periods with any precipitation were removed by the combined quality tests.

Table 3 presents the final amount of data that is left for analysis. From the EC system, only 29 % of the original 30-minute CO_2 data remains. For the FG system, more than half of the 30-minute data remains (58 % for CO_2 and 55 % for CH_4). Nor are there any long breaks in data from the FG system. For method comparison purposes, it is required that both systems have valid data at a given time. Combining the quality tests for the two methods for CO_2 results in a total of 27 % left for analysis. For all cases, more nighttime than daytime data was removed, which is expected based on the EC method assumptions of turbulent conditions.

Table 3: Percent of 30-minute data remaining for each method and for method comparison (CO_2) and for application of the FG method (CH_4). Day and night percentages are out of the total day/night values total.

Left for analysis	Total	Day	Night
EC CO_2	29 %	31 %	26 %
FG CO_2	58 %	69 %	43 %
Both EC & FG CO_2	27 %	30 %	23 %
FG CH_4	55 %	69 %	38 %

4.2 Meteorological conditions

Meteorological conditions for the study period are presented in Figure 8. Since the study covered less than a full year, no annual averages are presented. The average temperature for the study period was 9.8 degrees C with a minimum and maximum 30-minute average of -9.8 degrees C (March 22) and 32.3 degrees C (July 7) respectively. Total precipitation was 737 mm, which is slightly above the long-term annual mean (Lund et al., 2007). The distribution of rain was fairly uniformly spread throughout the year besides September (278 mm) and October (19 mm). As a result of little precipitation in mid-August (Figure 8 (b)), the water table depth (Figure 8 (c)) decreased to an annual-low of -0.16 m on August 24, only to return to close to zero after heavy rainfall in late August/early September. The average water table depth throughout the study period was -0.04 m, which is the same as the 2006-2009 average for DOY 100-300 at Fäjemyr (Lund et al., 2012). The average daily PAR (Figure 8 (d)) was 227 µmol m^{-2} s^{-1} and ranged between 4 µmol m^{-2} s^{-1} in February to 687 µmol m^{-2} s^{-1} in July.

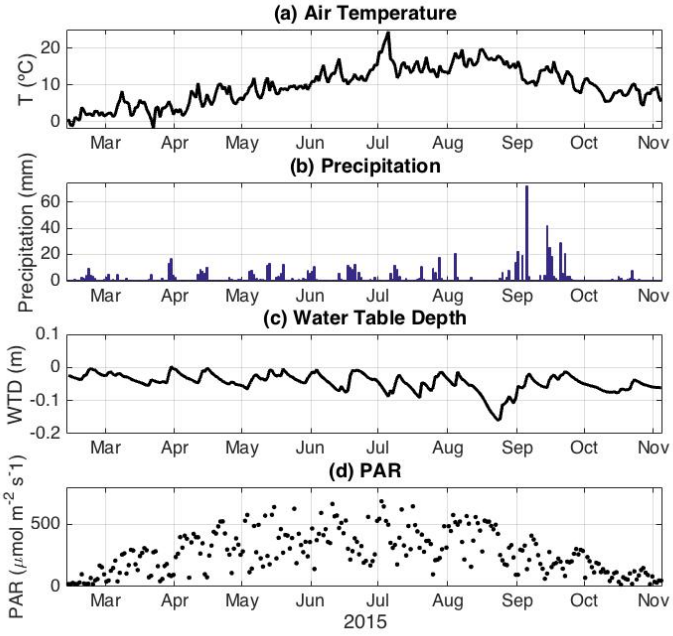

Figure 8: Meteorological conditions at Fäjemyr throughout the study period. Air temperature (a), precipitation (b), WTD (water table depth) (c) and PAR (d) are all daily averages. Negative water table depth indicates levels below the soil surface.

The prevailing wind direction was from the west-northwest and the average wind speed was 2.1 ms^{-1}, maximum average daily wind speed was 6.0 ms^{-1}, and the maximum average wind speed was 26.1 ms^{-1} (Figure 9).

For the EC method, 90 % of the cumulative contribution to turbulent fluxes came from within 130 m 89 % of the time and within 290 m 91 % of the time for quality checked data. Since the bog extends at least 290 m in all directions form the EC tower, this confirms that the EC footprint predominantly covers Fäjemyr's homogeneous peatland surface. Lund et al. (2007) tested the footprint at the same site

at Fäjemyr during different atmospheric stabilities and found that the fetch for the EC measurements were within the boundaries of the bog and therefore deemed all data reliable in terms of flux footprint. These findings are in line with a general rule of thumb for EC measurements, that the measurement height (3 m for Fäjemyr) should be about 100 times smaller than the desired fetch during turbulent conditions in order to avoid contamination of flux from bordering ecosystems (Horst & Weil, 1994). For stable conditions with very low $u*$, contamination from nearby ecosystems increases as the fetch could be as much as 5 times greater (Horst & Weil, 1994). This is yet another reason for excluding data with $u* < 0.1$ m s^{-1}.

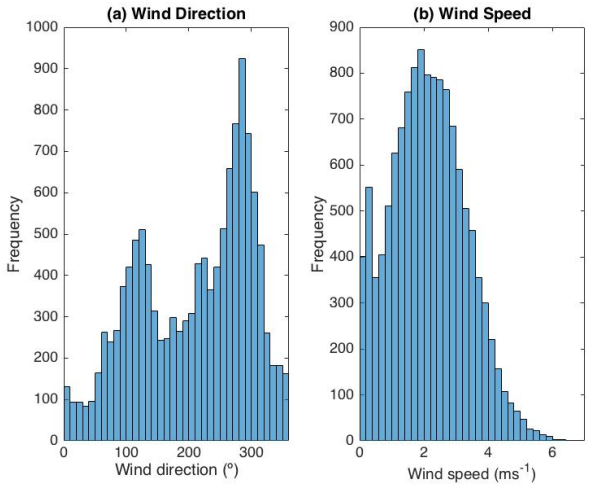

Figure 9: Distribution of wind direction (a) and wind speed (b) for 30-minute averages.

The flux footprint for the FG system is smaller than that of the EC system, since the lower intake level decreases the geometric mean measurement height. The height used for FG footprint purposes is 1.28 m ($\sqrt{0.55\ \text{m} * 3.00\ \text{m}}$). Using the same rule of thumb as above, the fetch of the FG method would be about 128 m, which is well within the boundaries of the bog. Assuming that the surface is uniform throughout the entire bog, the different flux footprints should not lead to differences in the resulting fluxes. However, this is a simplified assumption as in reality the vegetation, wetness and microtopography of Fäjemyr is not completely homogeneous. Yet it is comparatively homogeneous in comparison to other ecosystems. Nevertheless, it is more accurate to state that the differences in footprint size likely impact the method comparison, but to what extent and in what direction is difficult to say.

4.2.1 Friction Velocity u*

The friction velocity, $u*$, is an important measure of turbulence used for both EC and FG techniques, as sufficient mixing is required. The average value of $u*$ was 0.31 m s^{-1} (0.38 ms^{-1} for daytime and 0.23 ms^{-1} for nighttime). The distribution of 30-minute $u*$ averages is presented for both day and night conditions in Figure 10. As mentioned earlier, previous studies have found that for conditions of $u*$ below 0.1 m s^{-1}, nighttime CO_2 flux increases with $u*$ (e.g. Lund et al. 2007). Therefore all values below $u* = 0.1$ m s^{-1} (dashed line in Figure 10) were removed. Nighttime data was

removed to a larger extent than daytime data since stable conditions (low *u**) are more common during nights. 13 % of the dataset was removed (26 % out of all nighttime, 4 % of all daytime). A study from the same site at Fäjemyr removed 14 % of the annual data 2005/2006 using the same criteria (Lund et al., 2007).

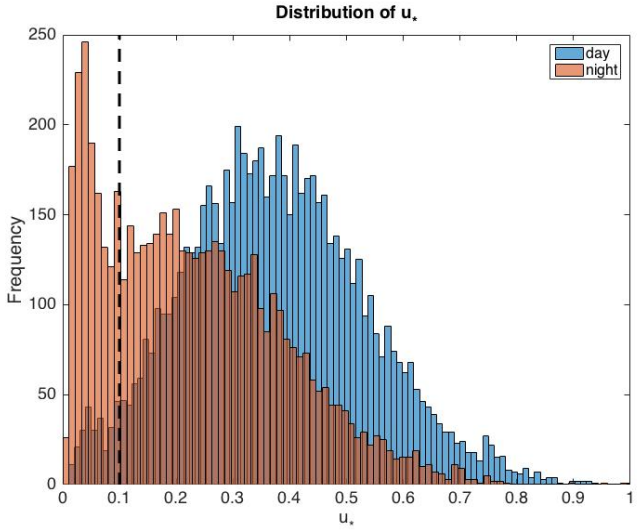

Figure 10: 30-minute *u** distribution for day and night. Values below *u**=0.1 (dashed line), which were removed due to insufficient turbulence, occurred during night.

A similar relationship as that found by Lund et al (2007) is presented in Figure 11. The EC setup used for that experiment was similar, but not identical to the current setup (e.g. a closed-path gas analyzer as opposed to an enclosed-path analyzer, and a Gill R3 sonic anemometer). However, the result confirms the positive relationship where CO_2flux increases with *u** below 0.1 m s^{-1} during growing season nighttime. The data presented in Figure 11 includes all growing season nighttime data, much of which was later removed by other quality tests. However, 19 % of the removed data due to low *u** was not removed by the Foken and Muader (2004) micrometeorological tests. This additional quality test increases the certainty that only the top-quality data remains for method comparison purposes.

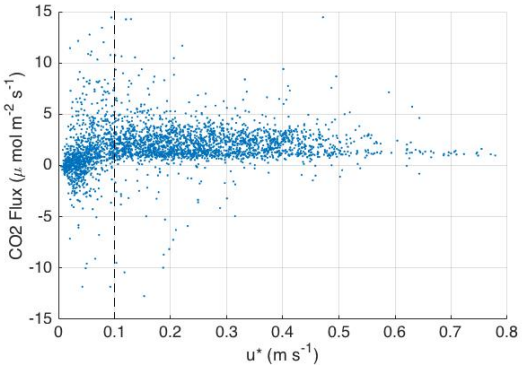

Figure 11: Scatter plot of growing season nighttime CO_2 flux vs. friction velocity (*u**). The dashed line indicates u* = 0.1 ms_{-1}.

4.3 CO_2 Concentrations

The 30-minute raw CO_2 concentrations are presented in Figure 12 (a) and (b). Since the FG system measured CO_2 concentration at two levels, only the upper level (3 m) is presented here to maintain consistency with the EC system, which also measured concentrations at a height of 3 m. Both systems capture the seasonal shift in concentration as photosynthesis dominates in the northern hemisphere summer. However, the decrease in concentration is greatly exaggerated for the EC system compared to previous years at Fäjemyr, whereas the magnitude of the FG system is in line with measured summer concentrations at Fäjemyr (M Lund 2016, personal communication, December). The shifts in EC CO_2 concentration after each time the analyzer was cleaned is visible in Figure 12 (a).

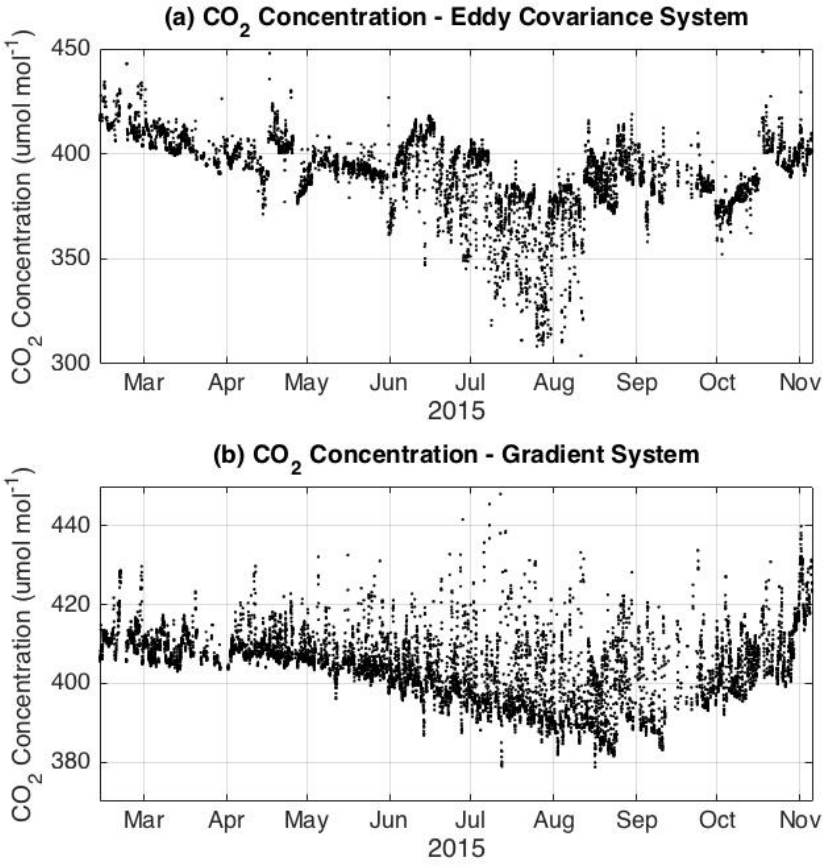

Figure 12: Recorded 30-minute CO_2 concentrations for the EC system (a) and the upper level of the FG system (b). Expected seasonal variation is seen in (b), whereas in (a), summertime concentrations are extremely low. LI-7200 cleaning dates are evident from the sudden concentration shifts in (a) (e.g. August 12 and October 16).

4.4 Effect of signal strength on resulting fluxes

Throughout June to mid-August, when LI-7200 signal quality was low, large differences in CO_2 flux were found (Figure 13 (a)). The CO_2 flux before and after the August 12 cleaning is visibly different between the two methods compared to the week following cleaning (Figure 13 (b) and (c)). The EC CO_2 flux before the cleaning

over-estimates the daytime CO_2 uptake compared to the FG method. After the cleaning, the daytime CO_2 uptake is similar for the two methods. Nighttime CO_2 flux are similar for both weeks.

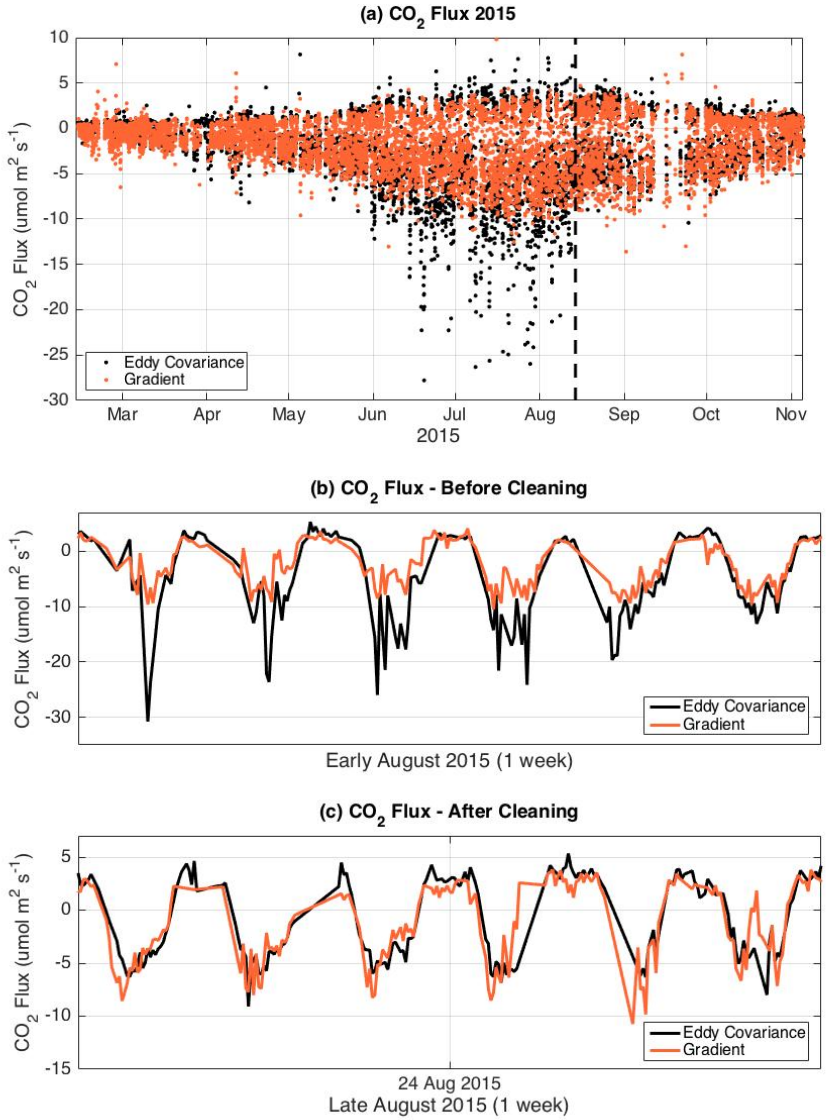

Figure 13: 30-minute CO_2 flux for both EC (before signal strength sorting) and FG (a). Daytime uptake (negative CO_2 flux) is much greater for EC compared to FG during the summer before the August 12 instrument cleaning (dashed line). FG CO_2 EC and FG CO_2 flux are compared for a one-week period in August before (b) and after (c) cleaning of the instrument, showing greater agreement in daytime flux after the cleaning.

Two one-month periods were investigated before and after the August 12 cleaning, which appeared to have the most significant impact on the EC signal strength and CO_2 flux.

Both periods had similar temperature ranges (Figure 14 (a) and (b)) and other meteorological conditions differed only slightly. However, the signal strengths (Figure 14 (c) and (d)) differed greatly between the two periods – both in magnitude (lower before cleaning) and in diurnal variation (greater before cleaning). As

expected, the EC CO_2 flux differed greatly from the FG CO_2 flux before the cleaning, especially during mid-day. This is seen by very low minimums in Figure 14 (e). Nighttime fluxes appear to be similar in magnitude. The main difference after the gas analyzer was cleaned on August 12 was that daytime EC CO_2 uptakes were lower, and close to the FG CO_2 flux. Regression analysis confirmed that the methods perform more alike after August 12 ($R^2 = 0.86$, slope = 0.91) compared to before cleaning ($R^2 = 0.69$, slope = 0.53).

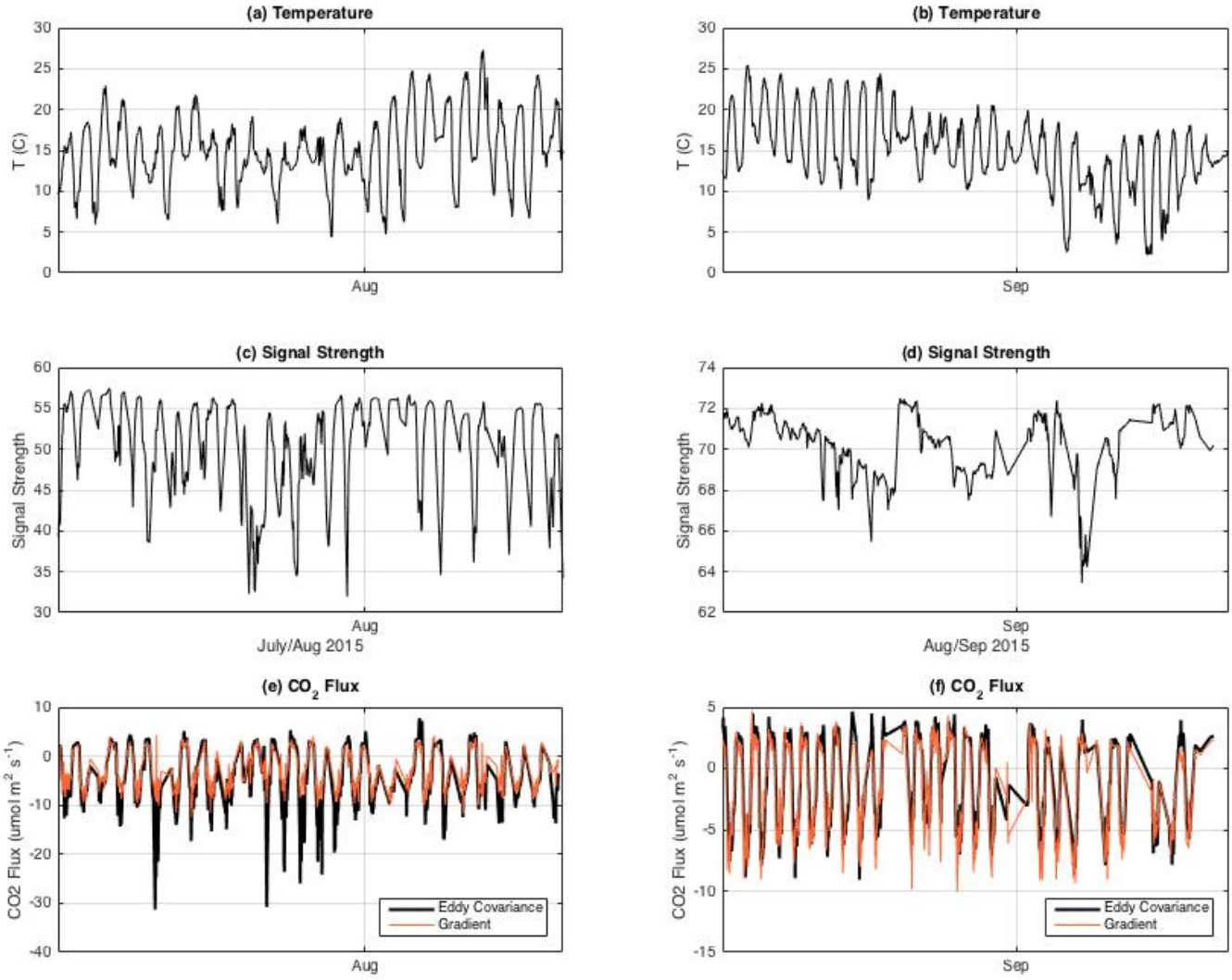

Figure 14: Comparing both methods' 30-minute CO_2 flux for a 1-month period before (left) and after (right) cleaning. Temperature and signal strength are shown before (a, c) and after (b, d) cleaning. Time series comparing the CO_2 flux before (c) and after (d) are shown as well. Only quality checked data is presented in the figure.

The conclusion made by observations of Figure 14 is that for the purpose of comparing the two measurement techniques, removing data based on signal strength quality was a necessary step. Also, the way signal strength was removed using dual criteria (both signal strength magnitude and daily standard deviation) seems to have been the most effective choice as there is no clear signal strength threshold for sorting good from bad data.

The magnitude of the removed EC CO_2 flux differs greatly from the corresponding FG CO_2 flux (Figure 13 (a)). Summer peak daily uptakes were around 10 µmol m^{-2} s^{-1} for the FG method whereas the removed EC fluxes for the same period were twice as high. During periods of both low and high flux, the methods yield similar magnitudes of CO_2 flux (for periods where both methods are quality checked). The magnitudes of the quality checked EC and FG CO_2 flux (both before and during growing season) correspond well with CO_2 flux magnitudes from a previous study at Fäjemyr by Lund et al. (2007) using a similar EC technique (e.g. a closed-path gas analyzer as opposed to an enclosed-path analyzer, and a Gill R3 sonic anemometer). Although this alone does not confirm that the removed EC summer CO_2 flux is indeed inaccurate, or that the FG CO_2 flux magnitudes are correct, the fact that both methods' magnitudes agree with each other and with a previous comparable study is a good indication.

When comparing the entire study period with or without low quality signal strength, it is again evident that the extremely high summer CO_2 uptake calculated by the EC method differ from the 1:1 line and thereby shifts the slope quite a lot (Figure 15). Once low quality signal strengths were removed, the slope changed from 0.58 to 0.88, and the R^2 value changed from 0.68 to 0.83.

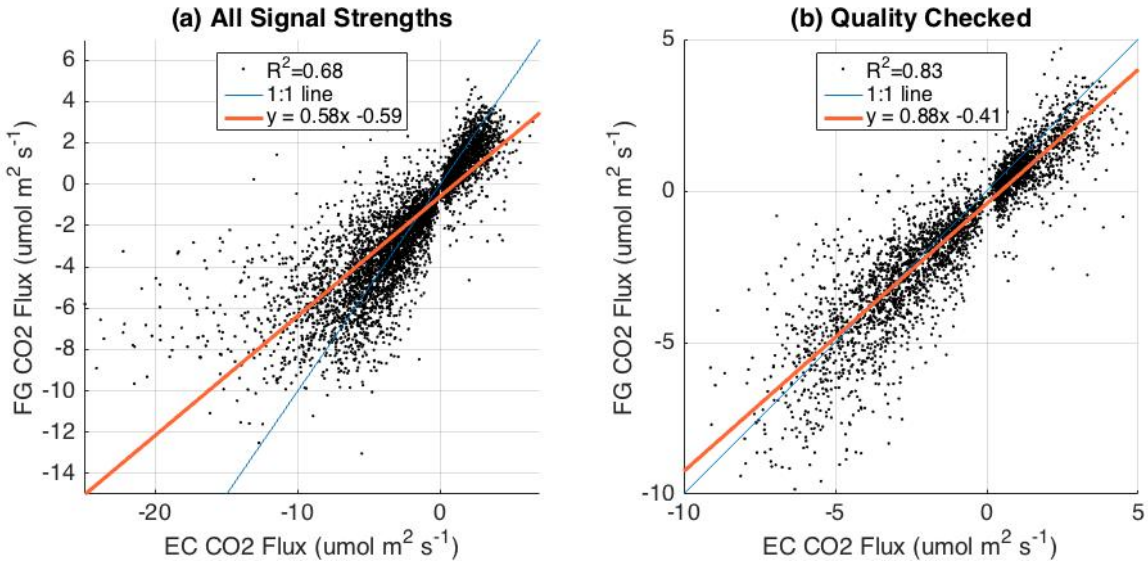

Figure 15: Scatter plots of FG vs. EC CO_2 flux for before (a) and after (b) signal strength quality check. Linear regression lines (red) approaches the 1:1 line (blue) after data was filtered for low-quality signal strength.

4.5 Gap-filled and cumulative CO_2 flux

Gap filled CO_2 flux for both methods allow for comparison of the seasonal variation in flux as well as calculating cumulative sums of CO_2 flux. The 7-day running mean daily CO_2 flux is shown in Figure 16 for both methods. The CO_2 flux for June to mid-August is the same for both methods as the EC gap was filled using FG CO_2 flux. Therefore, this specific time-period is difficult to analyze. Besides the summer gap, the FG shows more negative CO_2 flux (i.e. greater net uptake) than that of the EC method throughout the entire period. Although the magnitude differs, the methods seem to capture the same seasonal variation as well as shorter fluctuations on the time-scale of weeks (Figure 16). EC CO_2 flux are positive (CO_2 release) during the start and the end of the study period, whereas the corresponding FG are negative.

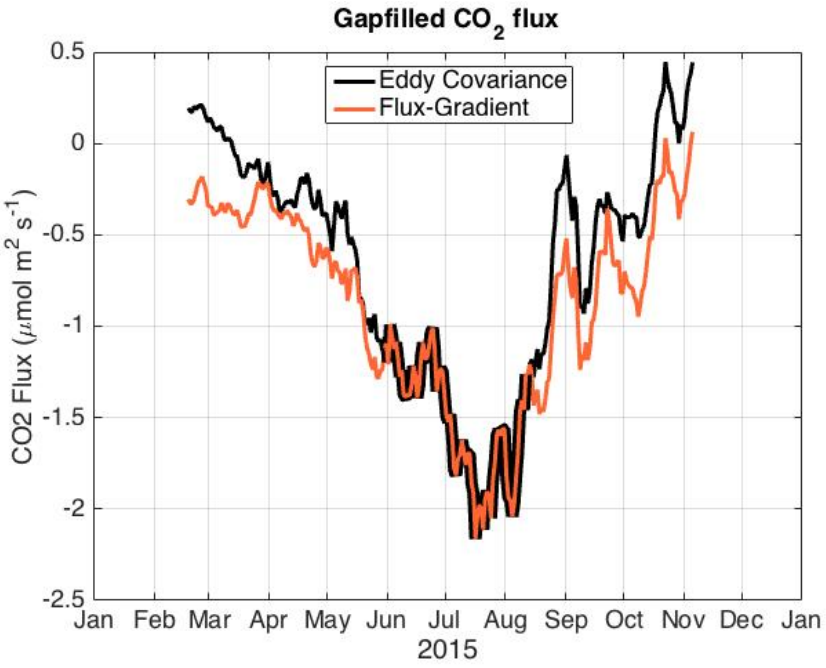

Figure 16: 7-day running mean daily CO_2 flux for each method (EC black, FG red). The EC summer gap (June 1 – August 12) was filled with FG data. Both methods capture the seasonal variation, but the magnitude varies slightly (greater net CO_2 uptake for FG).

As already inferred by Figure 16, the cumulative CO_2 flux also differ between the methods, with FG showing a stronger sink effect than the EC results. Figure 17 confirms that more C is sequestered for the FG method compared to the EC method. The net CO_2 balance resulted in –178 g C m^{-2} and -236 g C m^{-2} for EC and FG respectively (58 g C m^{-2} difference, or 28 % difference). If the EC method had been valid during the summer gap as well, the difference would likely have been even greater as EC was higher than FG the remaining part of the study period. The methods seem to differ the most in February-March and October-November, based on both Figure 16 (positive EC, negative FG) and Figure 17 (positive slope EC, negative slope FG).

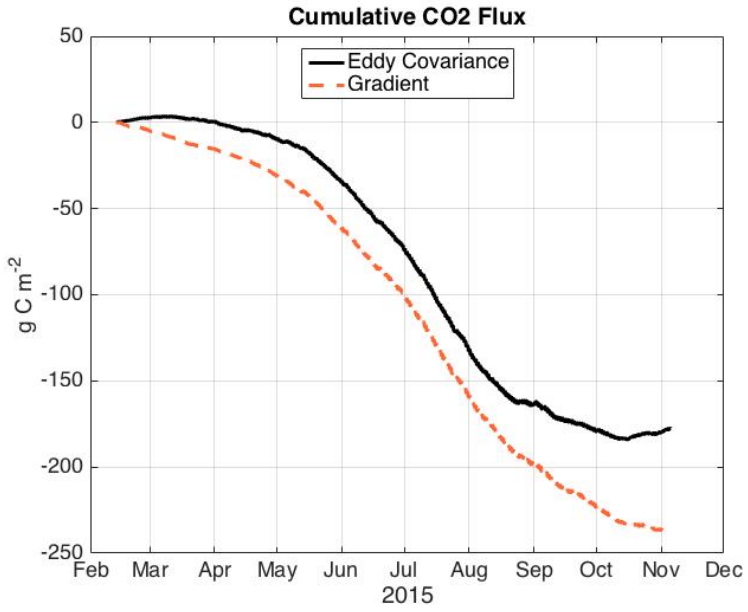

Figure 17: Cumulative CO_2 flux for both methods throughout the study period. The summer gap (June 1-August 12) in EC CO_2 flux was filled with FG data.

Compared to previous years at Fäjemyr, the cumulative CO_2 flux for both methods is comparable to other years with similar hydrological conditions (Lund et al., 2012). Lund et al. (2012) found that during the same time-period as this study (mid-February to early November), the cumulative CO_2 uptake was much smaller for two years with extended drought periods (defined as water table depth (WTD) < -10 cm) compared to wetter years. For this study, only a few days in August were that dry (compared to 49 and 91 consecutive days in the dry years of 2006 and 2008, respectively). Although the non-complete year makes quantitative comparison to other studies more difficult, the greater cumulative CO_2 uptake found during the wetter years by Lund et al. (2012) is comparable to the relatively large cumulative CO_2 uptake of both methods during this study.

Cumulative monthly CO_2 flux (g C m^{-2}) is shown in Figure 18. February and November are not full months as the study period began February 12 and ended November 5. For June and July, only FG data is shown, as the only data available for EC is the gap-filled CO_2 flux data. Cumulative August EC CO_2 flux partially consists of gap-filled FG CO_2 flux (Aug 1-12). For all 8 months with comparable cumulative flux, the FG method results in a greater CO_2 sink compared to EC. Both the actual difference and the relative difference is greater during early spring/late fall when the EC magnitudes are the smallest, which indicates that the methods perform more similar cumulative sums during the warmer/lighter months when the flux magnitude is higher compared to the colder/darker months when the flux magnitude is lower. The standard deviations of daily CO_2 flux for each month are much smaller than the difference between methods, which rules out random differences being the cause of these differences in monthly sums.

The greatest monthly cumulative CO_2 flux uptake and release of was -56.5 g C m^{-2} (FG, July) and +2.9 g C m^{-2} (EC, February) respectively. October differed the most

between methods (12.3 g C m^{-2}) and April differed the least between methods (5.1 g C m^{-2}), not counting the partial months of February and November.

The explanation for the methods' difference in both total cumulative CO_2 flux and monthly CO_2 flux can be found in Figure 19, where daytime and nighttime cumulative sums are plotted side by side. Monthly daytime cumulative sums (Figure 19 (a)) are similar in magnitude for both methods. On average the percent difference is 4 %. The cumulative sum for all months combined is -351 g C m^{-2} (EC) and -364 g C m^{-2} (FG). For nighttime, however, there are large differences (Figure 19 (b)). EC is higher than FG for all comparable months, and the total percent difference is 30 %. The cumulative nighttime difference for the study period (excluding the summer gap) is 45 g C m^{-2} (172 g C m^{-2} EC, 127 g C m^{-2} FG). Nighttime differences account for 80 % of the total difference between methods.

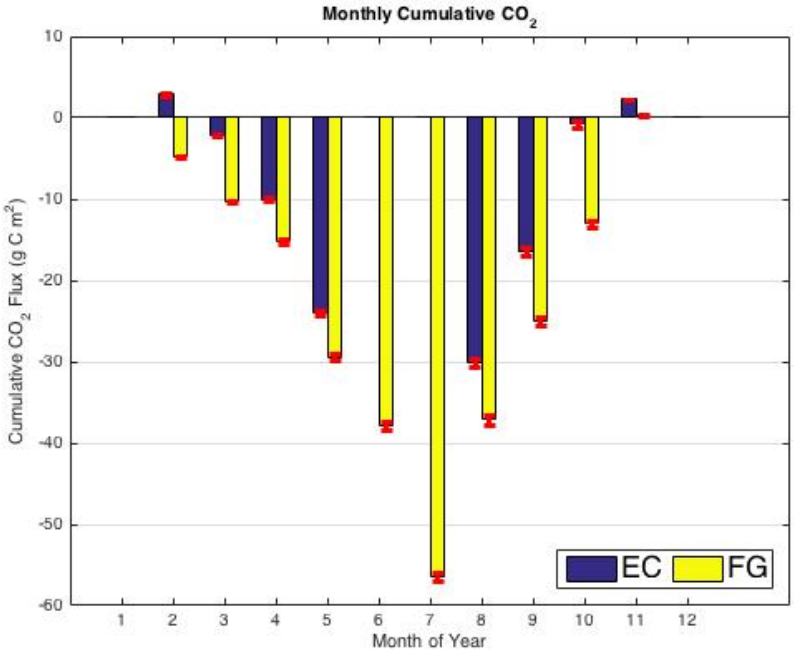

Figure 18: Cumulative monthly CO_2 flux (g C m^{-2}) for the entire study period in 2015 using quality tested and gap-filled data (FG CO_2 flux was used to fill EC gap August 1-12). Negative values indicate C uptake. Monthly standard deviations (based on daily flux) are shown for each month and method.

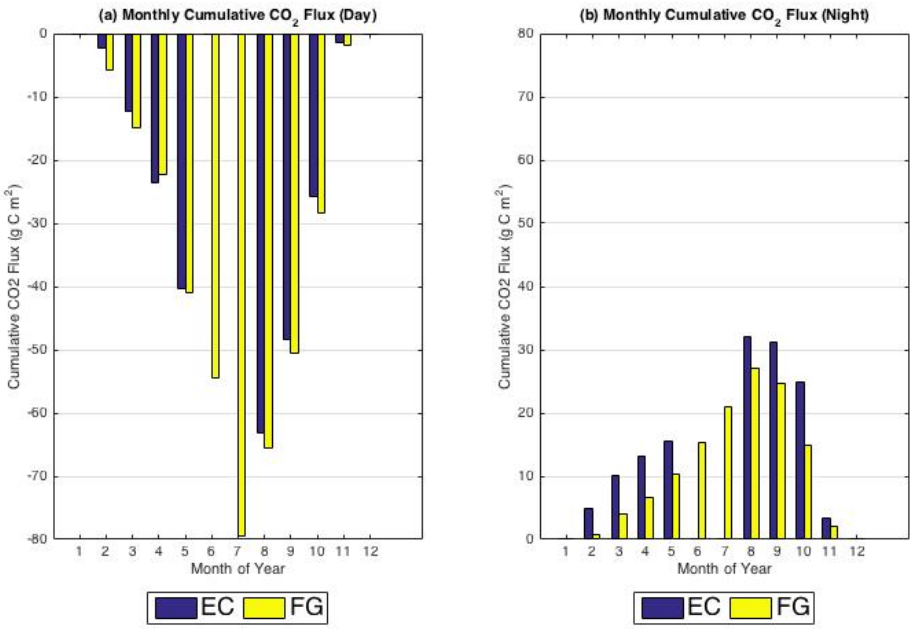

Figure 19: Cumulative monthly CO_2 flux (g C m^{-2}) for all daytime (a) and nighttime (b) throughout the study period using quality tested and gap-filled data (FG CO_2 flux was used to fill EC summer gap). Negative values indicate C uptake.

Analysis of the total time series of 30-minute gap-filled CO_2 flux for both EC and FG revealed that nighttime CO_2 release is greater for EC than for FG – both for periods with mostly measured data and for periods with mostly gap-filled data. A sample-period of 5 days in October is shown in Figure 20, where the nighttime difference is clear. Although the difference is not always as large as in Figure 19, the many small nighttime differences add up to large monthly and total cumulative difference.

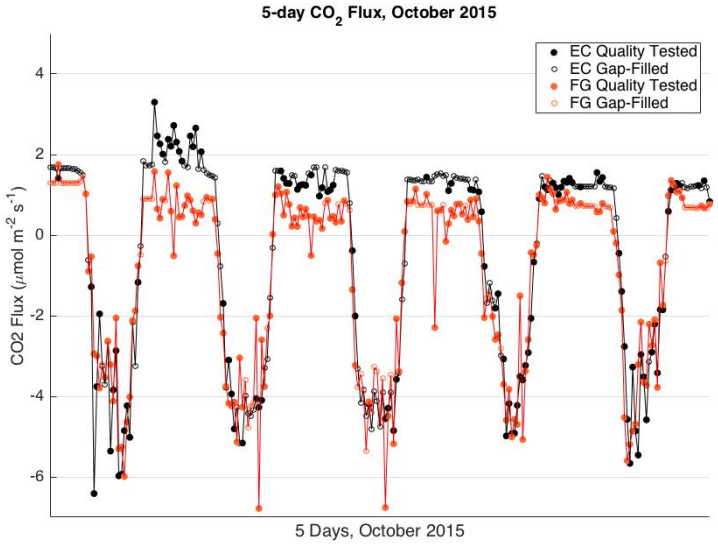

Figure 20: A 5-day period in October showing CO_2 flux for the two methods. Nighttime CO_2 flux is consistently greater for the EC method (black) compared to the FG method (red). Gaps in the quality tested data have been gap-filled.

Considering the difference in nighttime flux estimates between methods, it also makes sense that periods with more nighttime (e.g. Feb-Apr and October-November) differ more than months with more daytime (e.g. May), which was seen in Figure 18 and 20.

4.6 Method Comparison

In general, there is good agreement between the EC and FG methods regarding CO_2 flux. For all quality tested values (i.e. only measured data - no gap-filled data), the linear regression line has a slope of 0.88 and the R^2 value is 0.83 (Figure 15 (b)). Various conditions were tested in order to determine whether or not the agreement between the methods changed during certain conditions.

4.6.1 PAR

Method performance during different PAR-values (daytime only) during time periods ranging from a few days to several months was investigated. Data were divided into two groups within each time period based on PAR values (e.g. highest 10, 25 and 50 % vs lowest 10, 25 and 50 % respectively) No differences between methods were found using linear regression analysis, suggesting that both methods capture different times of day (e.g. morning, mid-day, afternoon) similarly. Also, the lack of difference between methods suggests that different cloud-cover conditions (e.g. sunny vs cloudy) does not impact the consistency between the methods either.

4.6.2 Turbulence

The median of u^* during nighttime was 0.28 m s^{-1}. For nighttime and u^* below the median, there was worse agreement (R^2=0.50, slope=0.65) than for nighttime and u^* > 0.28 m s^{-1} (R^2=0.52, slope=0.78). This is expected since greater turbulence (high u^*) promotes better performance of EC and FG method. Even though the lowest u^* were removed, less turbulent nighttime conditions likely causes worse agreement between methods compared to turbulent daytime conditions. There was no difference in method agreement depending on u^* during daytime conditions.

4.6.3 Wind

The surrounding vegetation and surface properties were assumed to be homogeneous for this study, as that is one of the underlying assumptions for EC measurements. However, in practice this is not exactly the case. E.g., Figure 21 shows that the scattered small pine trees are not scattered symmetrically around the EC mast. Unsymmetrical distribution of the pine trees could in theory affect both the source/sink of CO_2 depending on wind direction, as well as generating more turbulent flow not included in the profile function used for FG flux. Different wind directions were therefore tested to make sure that there were no great variations in CO_2 flux between methods depending on wind direction.

Figure 21: Aerial photograph over Fäjemyr (Google Maps, 2016) showing the rather (but not perfectly) uniform vegetation surrounding the EC mast. The red circle indicates the location of the EC tower. The bog extends nearly 300 m in all directions around the EC tower.

The magnitude of CO_2 flux varied slightly depending on wind direction (e.g. higher uptake for westerly winds as that is the predominant wind direction during late spring and summer). However, as expected, there was little variation between the two methods depending on wind direction. Linear regression analysis was performed on scatter plots of EC and FG for winds divided into both 45 degree intervals and 90 degree intervals (Table 4). Analysis of R^2 and slope for the two methods indicate that the methods yield high R^2 and slope for all wind directions (highest: SW $R^2 = 0.85$, slope = 0.99, lowest: NW $R^2 = 0.78$, slope = 0.81). Southerly winds resulted in slightly better agreement compared to northerly winds. Although the tree density is noticeably higher south of the EC tower compared to north of the tower, it is difficult to attribute the difference to that fact – especially since the agreement between methods is high for both wind directions. Different wind speeds were also tested, but strong agreement between methods were found for all scenarios.

Table 4: Results from linear regression analysis of FG vs. EC for varying wind directions (45 and 90 degree intervals) for day, night, and all. R^2, slope and number of records, N, are presented for each wind direction interval.

45 degree intervals	All (R^2/Slope/N)	Night (R^2/Slope/N)	Day (R^2/Slope/N)
N	0.78/0.88/139	0.80/0.98/13	0.7/0.82/126
NE	0.79/0.80/98	0.29/0.52/27	0.63/0.71/71
E	0.85/0.87/633	0.54/0.70/340	0.70/0.83/293
SE	0.82/0.85/511	0.65/0.91/140	0.69/0.86/371
S	0.84/0.98/339	0.47/0.69/169	0.72/0.98/170
SW	0.85/0.99/504	0.56/0.90/193	0.77/1/311
W	0.83/0.91/682	0.29/0.58/288	0.63/0.89/394
NW	0.78/0.81/527	0.61/0.29/114	0.63/0.78/413

90 degree intervals	All (R^2/Slope/N)	Night (R^2/Slope/N)	Day (R^2/Slope/N)
N	0.75/0.84/345	0.57/1/39	0.64/0.80/306
E	0.85/0.85/1033	0.56/0.75/467	0.69/0.83/566
S	0.83/0.94/808	0.58/0.82/325	0.71/0.94/483
W	0.83/0.90/1247	0.32/0.63/453	0.68/0.91/794

4.6.4 Footprint differences

Considering that the measurement heights are different for the two methods, the resulting flux footprints are also different. For footprint purposes, the measurement height for the FG system is calculated as the arithmetic mean for stable conditions (1.78 m) and geometric mean for neutral and unstable conditions (1.28 m). Considering that the measurement height for the EC system is 3.00 m, the height differences result in quite large differences in footprint extent and peak contribution.

Had the vegetation not been sufficiently uniform in all directions at Fäjemyr, larger differences in between methods likely would have been detected for different wind directions due to contamination from various flux contributors from the underlying surface. However, analysis of different wind directions suggests that overall (day and night), the different footprints does not have a large impact on method agreement. If anything, there is greater variation in method agreement (i.e. varying R^2 and slope) depending on wind direction for nighttime compared to daytime. This could possibly be explained by stable nighttime conditions exaggerating any footprint differences as the fetch of the footprint increases with stability (Horst & Weil, 1994). But more likely, this is a result of random variation being more evident for certain wind directions, where there are few nighttime data points available for comparison.

4.6.5 Temperature

Impact of temperature on method performance was more difficult to test as differences could be caused by other factors such as seasonal or day/night effects. The methods agreed better for the warmest 25 % compared to the coldest 25 %. However, in order to rule out effects from day/nigh or time of year, eight scenarios were tested. The study period was divided into warm and cold months:

Warm: May, August, September
Cold: February, March, April, October, November

Further, day and night were tested separately. And finally, the highest vs. the lowest 25 % temperatures were tested within each group.

The methods agree better during daytime conditions, and during both the warm months and the cold months, the agreements is better for the warmer 25 % compared to the colder 25 % (Table 5). During nighttime, agreement between methods is significantly worse. Temperature does not seem to impact the agreement between methods during nighttime. If anything, colder nights during the warm months agree better than the warmer nights during the same months.

Table 5: Results of linear regression analysis of EC and FG CO_2 flux during warm/cold months, day/night and warm/cold 30-minute values.

Time of year	Day/Night	Warm/Cold 25%	T threshold (C)	Linear regression (R^2/slope)
Warm	Day	Warm	>17.6	0.59/0.94
Warm	Day	Cold	<11.8	0.6/0.76
Warm	Night	Warm	>14.2	0.01/-0.15
Warm	Night	Cold	<8.7	0.06/0.29
Cold	Day	Warm	>10.8	0.61/0.88
Cold	Day	Cold	<6.5	0.40/0.63
Cold	Night	Warm	>7.6	0.01/0.15
Cold	Night	Cold	<2.3	0.01/0.15

4.6.6 Day/Night

Throughout the entire study period, there is better method agreement during daytime than during daytime. EC consistently yields higher nighttime flux compared to FG. Figure 22 shows scatter plots of all quality tested measured CO_2 flux for daytime (a) and nighttime (b). Higher R^2 and slope (R^2 = 0.68, slope = 0.86) for daytime indicates that the methods perform more consistently (i.e. better agreement between methods) during daytime compared to nighttime (R^2 = 0.50, slope = 0.73).

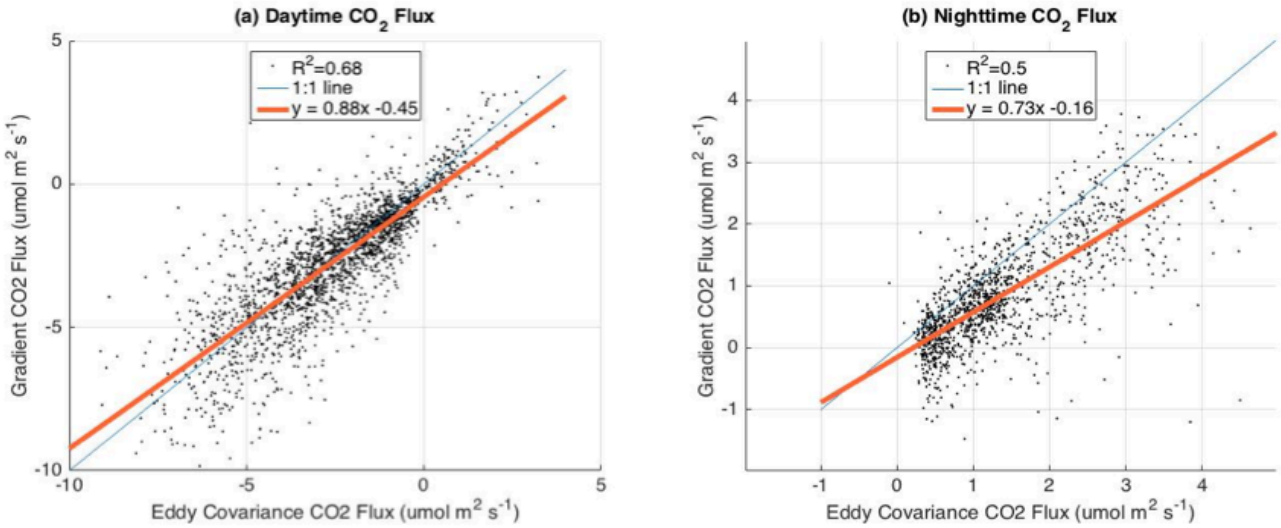

Figure 22: Scatter plot of all quality tested measured 30-minute CO_2 flux for both methods during daytime (a) and nighttime (b). The linear regression lines (red) deviates more from the 1:1 lines (blue) during nighttime, indicating worse agreement between methods during nighttime.

Diurnal CO_2 flux is shown in Figure 23 (measured data only). The study period was divided into the warmest months (May-September, average T = 12.0 ºC), characterized by high flux, and the coldest months (February-April and October-November, average T = 5.3 ºC), characterized by low flux. The average CO_2 flux for each hour of the day and for each method reveals that the nighttime difference between methods is relatively constant around 0.5 µmol $m^{-2}s^{-1}$ regardless of season. Considering that the magnitude of nighttime release is lower during the winter, the percent difference is also the greatest for these periods of low flux. The methods agree well during daytime throughout the entire study period, with closest agreement most often during the afternoons.

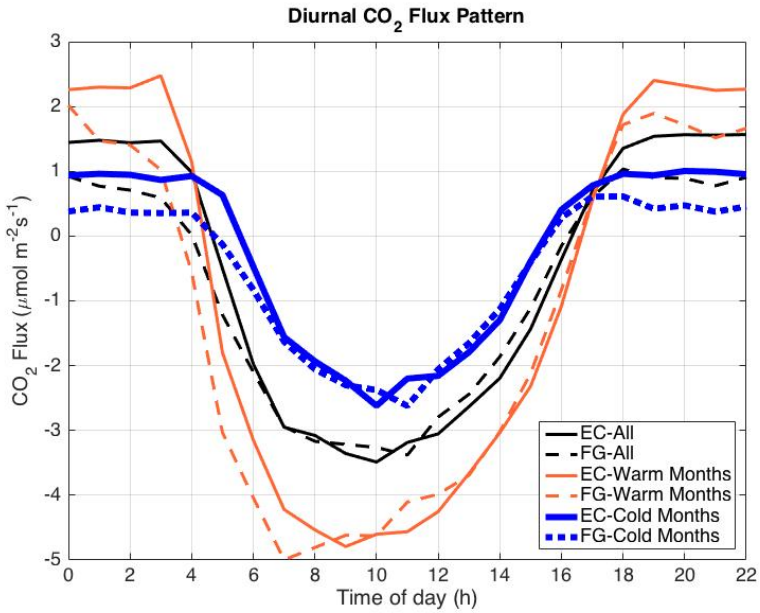

Figure 23: Average CO_2 flux for each hour of the day for the whole study period (black), for warm months (red, May-September) and for cold months (blue, February-April, October-November). Solid lines for the EC method and dashed lines for the FG method. Only quality checked measured CO_2 flux is included (summer period with bad signal strength was not included for either method).

4.7 Possible causes of flux differences

The strict quality checks in this study likely increases method agreement and makes it harder to find possible causes of differences in method performance. Some relationships may have been visible before e.g. the micrometeorological test for turbulent conditions removed much of the data. Also, the fact that more nighttime than daytime data was removed may have made nighttime relationships more difficult to detect.

For lower magnitudes of CO_2 flux, such as during winter and early spring, the measurement errors are relatively larger than during times of higher flux magnitudes. For FG, the turbulent diffusivity depends on both measurements of u^* and H. Lower wind speeds and higher stability (typical nighttime conditions) increases the uncertainty in turbulent diffusivities, which increases the error in estimated flux. Also, random variation has a greater impact on flux errors during periods of low flux magnitude. The detection limit for an EC system is often not better than 0.5-1 µmol $m^{-2}s^{-1}$ (P Vestin 2016, personal communication, December), and there is no support for FG measurements having better detection limits. This could explain why the methods differ more during nighttime and during times of flux magnitudes around 0-2 µmol $m^{-2}s^{-1}$ (e.g. early spring). Unfortunately, most of the summertime CO_2 flux was not valid for method comparison, but since flux magnitude is greater during the summer, a greater relative agreement could have been found if EC summer data had been valid. Support for such reasoning was found during periods of higher flux in e.g. May, August and September, where greater relative agreement was found compared to times of lower flux (e.g. February-April). The fewer nighttime values during summertime would also have decreased the systematic differences in cumulative sums caused largely from nighttime differences.

When the CO_2 concentration gradients approached zero, there was worse agreement between methods, which is not surprising as non-resolvable gradients imply non-resolvable flux (i.e. flux close to zero) according to the flux-gradient equation (Laubach et al., 2016). The average difference in CO_2 concentration between levels was 0.86 ppm. The gas analyzer precision was specified as 0.04 ppm (100s, 1 std dev). It is expected that gradients closer to zero result in less accurate flux estimates. When the concentration differences were less than the gradient resolution ($\sqrt{2} \bullet 0.04$ ppm), the agreement between methods was poor ($R^2 = 0.14$, slope = 0.07, n = 149). Differences smaller than the gradient resolution cannot be considered significantly different from zero (Laubach et al., 2016). Even a noticeable difference in method agreement was found for e.g. concentration difference < 0.28 ppm, the lower quartile value ($R^2 = 0.51$, slope = 0.37, n = 884), compared to concentration difference > 1.15 ppm, the upper quartile value ($R^2 = 0.89$, slope = 1.00, n = 884). Data was not removed when the gradients were small since many repeated measurements over time, even if the flux is non-resolvable, still contribute to a better resolved mean flux (Laubach et al., 2016).

Undersampling of concentration is also a likely explanation to observed differences between methods, as only one level of the FG system is measured at a time. Rapid changes in environmental conditions such as turbulence, PAR (e.g. due to cloudiness), wind speed/direction, sunrise/sunset can impact the measurements at the different heights differently, causing too large or too small CO_2 concentration gradients. Had concentrations instead been recorded simultaneously at both levels, changes in the ecosystem would have been detected more accurately by the FG system and errors associated with rapidly changing conditions would have decreased (P Vestin & Meelis Mölder 2016, personal communication, December). In theory, the conditions most suitable for this FG setup are therefore daytime conditions with clear skies (rather constant PAR), with constant wind speeds and constant wind direction. Yet good agreement was found even for less than ideal conditions, suggesting that the FG method is reliable for a wide range of environmental conditions found at Fäjemyr.

The contribution of error in flux (both CO_2 and CH_4) was greater for error in diffusivity compared to error in gradients for Fäjemyr. The opposite case was found by Sundqvist et al. (2015). However, the experiment setup was different (e.g. greater gradient height differences in Sundqvist et al.) and the ecosystem was different as well (coniferous forest). For the same study, weak daytime gradients resulted in much daytime data removal, whereas nighttime data was accepted. This was also the opposite case compared to Fäjemyr, where more daytime data was valid.

Based on the findings from this study, the FG method agrees well with the EC method during the daytime and during warmer months (i.e. higher flux magnitudes) compared to nighttime and during colder months. The worse agreement during nighttime does not seem to be affected by temperature, but is likely related to stronger atmospheric stability during nighttime. These findings are in agreement with the fact that EC measurements are more reliable for warm periods, during daytime with turbulent conditions (Burba & Anderson, 2012). The worse relative agreement during winter and early spring are likely due to lower magnitude fluxes, for which the effects of random variations is the greatest.

4.8 Applicability of FG for CH_4 flux

Since EC is considered a reliable method for flux estimates at relatively homogeneous sites such as Fäjemyr, and the FG technique largely agrees with EC for CO_2 flux, there is support for claiming that the FG technique is also applicable for CH_4 flux estimates at Fäjemyr. Following the same reasoning as for CO_2 flux, the CH_4 flux should be most reliable during warm periods and daytime, when sufficient atmospheric mixing is present and flux magnitudes are large. Since the diurnal variation in CH_4 flux is less than diurnal CO_2 flux, the uncertainty associated with daily average CH_4 flux should be less than for CO_2 flux. Especially during the summer months, when nights are shorter and flux magnitudes are greater, the daily average CH_4 flux should be most accurate. Since these favorable conditions for the FG method coincide with the time of year where CH_4 flux are greatest in magnitude, the annual cumulative sums will largely originate from periods of higher confidence in the FG method.

4.9 CH_4 Results

The CH_4 concentrations at the upper intake level (3 m) for the entire study period (quality tested data only) are shown in Figure 24 (a). The mean concentration was 1.95 µmol mol^{-1} and the concentration ranged between 1.9-2.0 µmol mol^{-1} throughout most of the period. There is little seasonal variation in CH_4 concentration compared to the CO_2 concentrations (slightly lower during the summer). The mean concentration from the lower intake level (0.55 m) was the same as for the upper level throughout the study (1/1000 µmolmol^{-1} higher).

Since only the FG measured CH_4 data, more data remained after all quality tests. 55 % of all 30-minute values were accepted (twice as much as for the CO_2 method comparison), and 89 % (236 of 266) of daily averages were accepted (the remaining daily gaps were linearly interpolated).

Quality tested 30-minute and daily average CH_4 flux are presented in Figure 24 (b) and (c), respectively. The seasonal variation with low flux during winter and spring, and higher flux during summer and fall is also expected based on previous studies at Fäjemyr and other similar peatlands (Limpens et al., 2008; Lai, 2009; Bellisario, 1999; Lund et al., 2009). Peak summer flux was around 250 µmol m^{-2} hr^{-1} (daily average around 200 µmol m^{-2} hr^{-1}) and winter/early spring flux ranged between 0 and 50 µmol m^{-2} hr^{-1}.

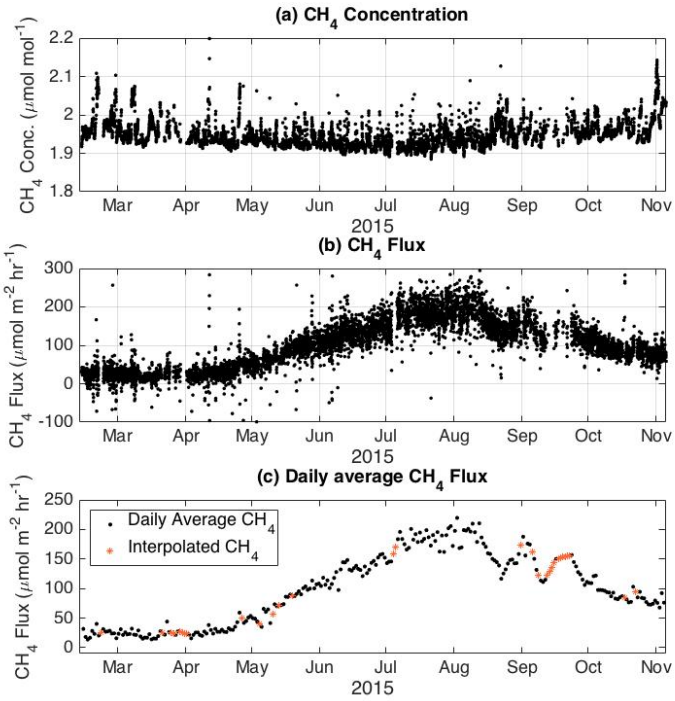

Figure 24: Quality checked 30-minute CH_4 concentration (a), flux (b) and daily average flux (c) for the whole study period. The data is rather continuous, resulting in few gaps. The gaps in daily CH_4 flux were filled using linear interpolation (red dots in(c)).

CH_4 flux in relation to environmental variables are shown in Figure 25. Seasonal temperatures (air T and soil T) follow a similar trend as CH_4 flux. Soil temperature at 20 cm depth most likely explains the CH_4 flux better than air temperature and 5 cm soil temperature, due to the smaller variations in temperature throughout the year. As an example, the peak in temperature (both air and soil temperature) in early July correspond with the small peak in CH_4 flux.

Water table depth (Figure 25 (c)) also seems to impact the CH_4 flux to some extent. The dry period in August caused the water table to drop to below -10 cm for several consecutive days, which coincided with a dip in CH_4 release. This is likely due to the unusually low water table allowing oxidation to take place instead of methane production as usual under anaerobic conditions (Limpens et al., 2008).

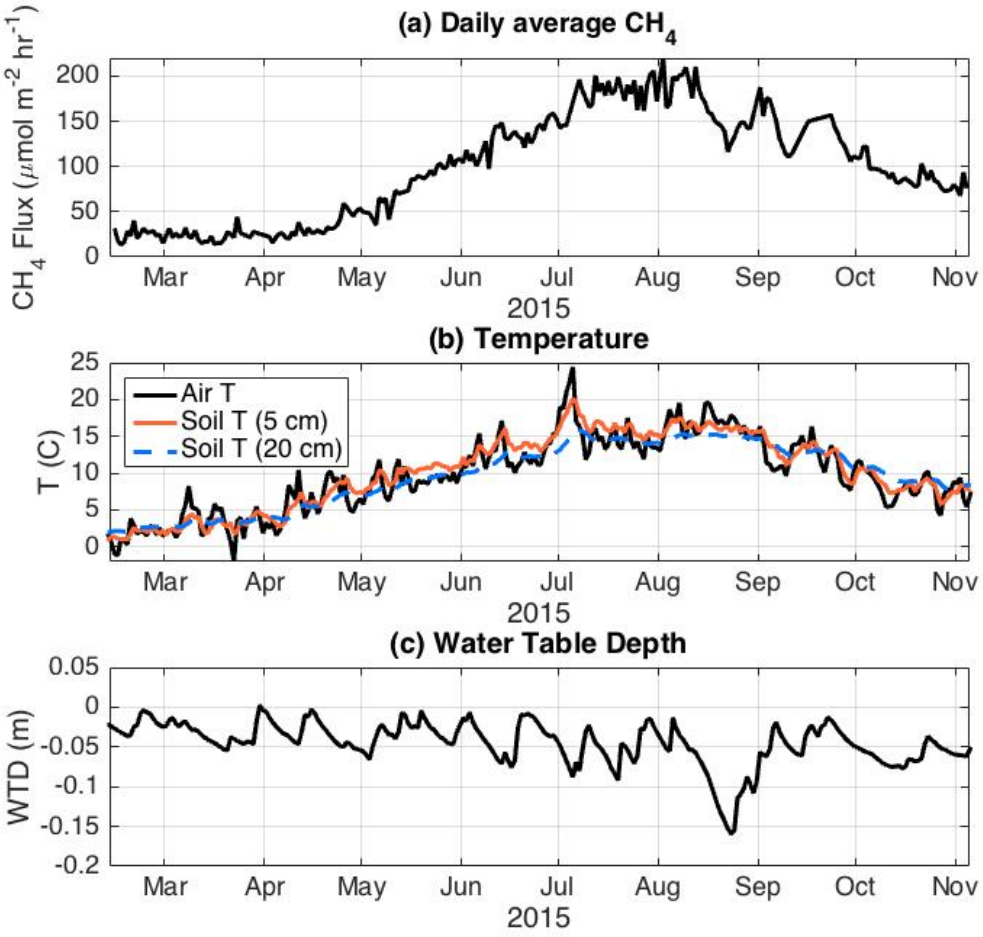

Figure 25: Daily average CH_4 flux including linear interpolation of gaps (a), daily soil temperature (5 cm and 20 cm) and air temperature (b), and daily water table depth (c).

Clear relationships are seen for temperature and CH_4 flux in Figure 26. 20 cm soil T showed the highest R^2 of 0.91. The scatter plots all resemble what is often found in methane studies, which is an additional argument for the applicability of the FG method for CH_4 flux purposes. Temperature relationships are often the most pronounced, sometimes exhibiting more of an exponential relationship instead of a linear relationship (e.g. Hargreaves et al., 2001; Rinne et al., 2007; Wille et al., 2008). The temperature relationship in this study seems to be somewhat exponential (e.g. Figure 26 (d)). CH_4 flux relationships with WTD is often less evident, but exerts a more nonlinear control on CH_4. Small variations in WTD may not be important above a certain level, but if conditions become dry enough, the CH_4 flux will drop (Christensen et al., 2003) as seen during the dry period in august (Figure 25 (a)).

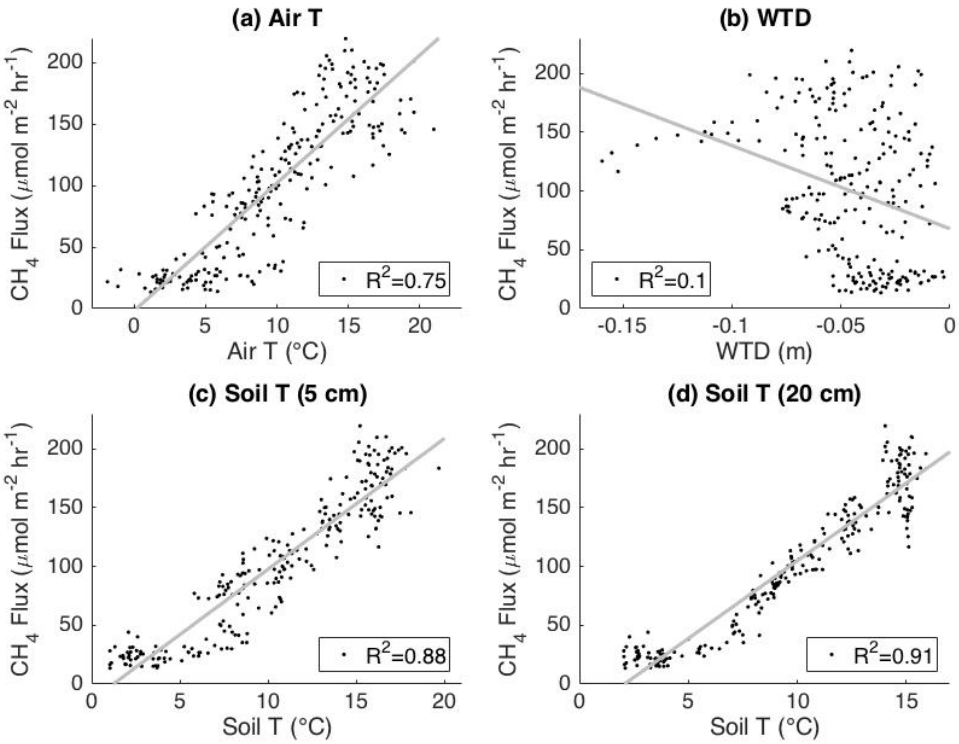

Figure 26: Scatter plots of daily CH_4 flux and air T (a), WTD (b), 5 cm soil T (c) and 20 cm soil T (d). Linear regression lines and R^2 are presented.

A small diurnal variation was found for CH_4 flux, which is presented in Figure 27. Daytime fluxes were higher than nighttime fluxes in general, with a diurnal peak in the late afternoon. The diurnal pattern was most evident during the summer months, when the flux magnitudes were the greatest and during the winter and early spring no clear variation was found (e.g. August diurnal variation compared to Feb-Mar variation, Figure 27 (a)).

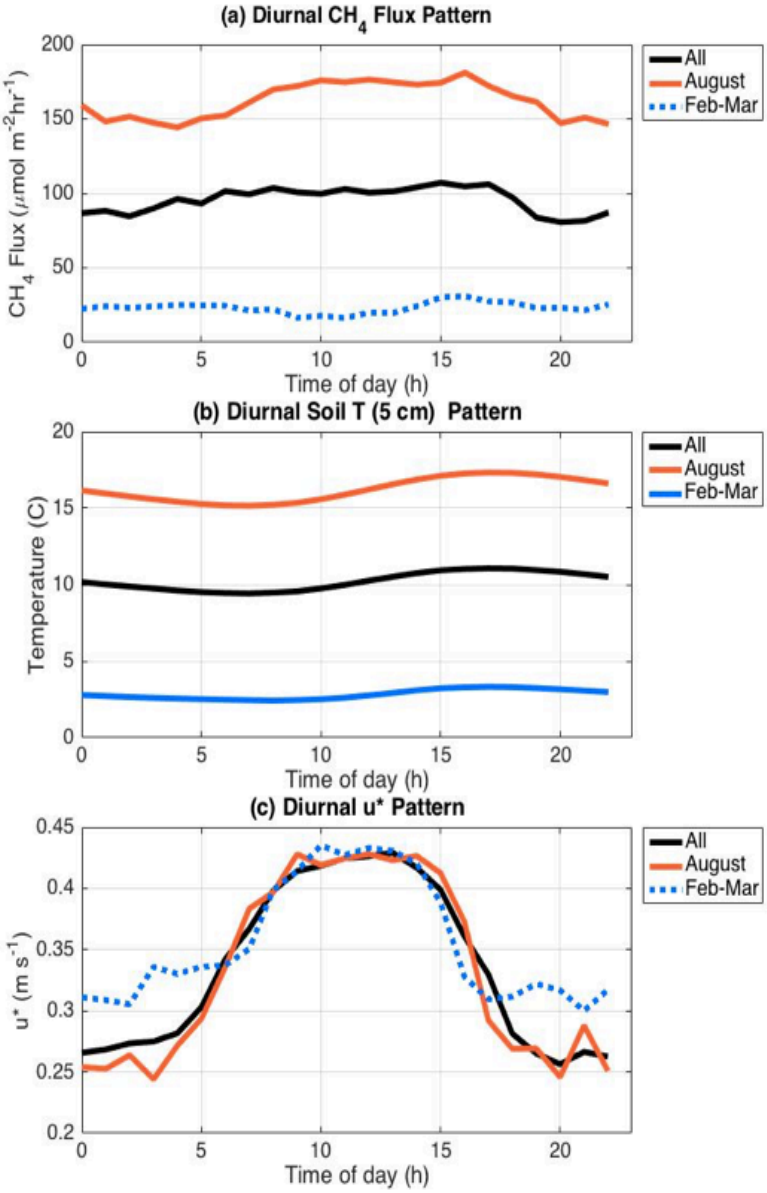

Figure 27: Diurnal CH_4 flux (a) for the entire study period, a period of high CH_4 flux (August), and a period of lower CH_4 flux (February-March). Diurnal soil temperatures and u^* for the same time periods are shown in (b) and (c) respectively.

Studies of similar sites have shown both diurnal patterns in CH_4 flux (Suyker et al., 1996; Kim et al., 1998) and lack of diurnal patterns (Rinne et al., 2007; Kormann et al., 2001). Causes of the diurnal pattern in CH_4 flux were investigated and two possible causes, soil temperature and friction velocity, are presented in Figure 27 (b) and (c), respectively. The temperature dependence has already been shown for seasonal patterns, but could possibly also impact CH_4 flux on the diurnal time scale. Both soil temperature at 5 cm depth and CH_4 flux peak around the same time in the afternoon and could therefore partly explain the observed diurnal variation. The more turbulent daytime conditions (shown by friction velocity, Figure 27 (c)) may also be more favorable land-atmosphere CH_4 exchange. However, the processes controlling CH_4 release are rather complex and the observed diurnal variation is likely a combination of many factors. As an example, there are several ways in which CH_4 can be released to the atmosphere (e.g. diffusion, ebullition and plant-mediated transport) and the methane production and oxidation occurs at different depths and therefore

have temperature maximums at different times during the day. They also have varying sensitivity to temperature. Estimating the time it takes for CH_4 to be transported from the depth it was created to the atmosphere further complicates the matter. The above-mentioned challenges associated with CH_4 flux are some of the reasons why gap filling is difficult. There is currently no standardized method for CH_4 gap filling, but one common method is neutral networks (Dengel et al., 2013). Since the gaps were few in this study, and due to limited time, linear interpolation was satisfactory in order to infer the applicability of the FG method.

Compared to the CO_2 flux, which varies greatly between day and night, CH_4 flux remain more constant between day and night. Since micrometeorological techniques such as FG and EC have a substantial data loss during nighttime conditions, the uncertainty associated with the CH_4 daily average flux and annual cumulative flux is lower compared to e.g. CO_2. As the diurnal cycle decreases, the systematic error for daily averages decreases as well and leaves only the random uncertainty. Therefore, the FG technique is a suitable technique for CH_4 flux estimates on both shorter (i.e. days) and longer (i.e. years) timescales.

The cumulative CH_4 flux throughout the study period was 6.8 g C m^{-2}. Since the wintertime contribution to the cumulative annual CH_4 flux is small, the results found in this study can still be used for general comparison to other studies despite the missing winter months. Lund et al. (2009) used the automatic chambers technique to estimate CH_4 flux at Fäjemyr for one year (7 Feb 2008 – 6 Feb 2009) and found that the cumulative CH_4 flux ranged between 1.1 and 3.1 g C m-2 for 6 different chambers (highest flux for hollows, lowest flux for hummocks). However, the water table depth was extremely low during the summer (-10 to -20 cm throughout most of May-July) and higher CH_4 flux were expected for other years (Lund et al., 2009) since CH_4 exchange is often found to correlate with water table depth (Christensen et al., 2003).

Annual CH_4 flux for sites comparable to Fäjemyr range between 3-13 g C m^{-2} using both the chamber technique (Laine et al., 2007; Roulet et al., 2007; Nilsson et al., 2008) and EC technique (Rinne et al., 2007). During 2015, Fäjemyr places in the middle of this range instead of the lower end of the range found during an extremely dry year (Lund et al., 2009).

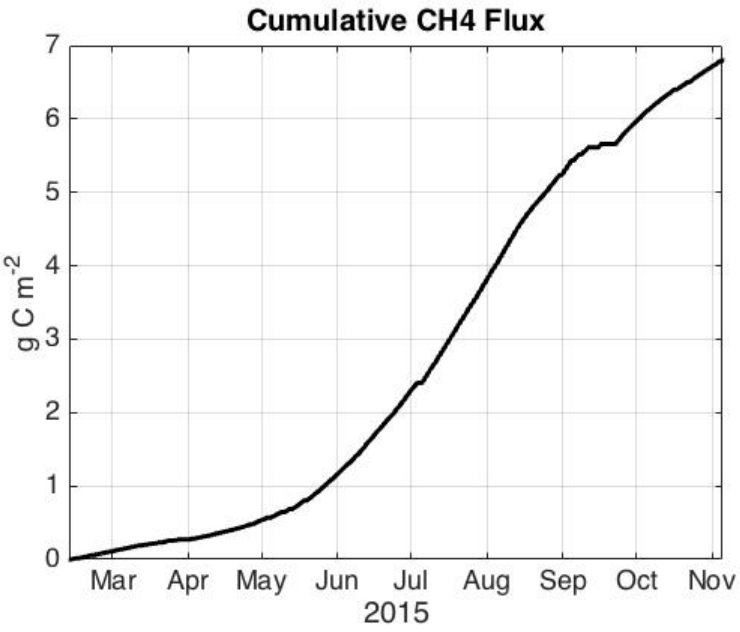

Figure 28: Cumulative fluxes of CH_4 estimated by the FG system throughout the study period.

The cumulative CH_4 flux is small, but not negligible, compared to CO_2 flux in terms of C budgets. However, the potency of CH_4 as a greenhouse gas greatly offsets much of the cooling effect by CO_2 sequestration, which makes CH_4 a major factor for radiative forcing effects by northern peatlands in the future. Accurately estimating both CO_2 and CH_4 flux for current and future climates is therefore key for improving global climate models.

5. Conclusion

In this study, the EC and FG techniques were compared using CO_2 in order to assess the applicability of the FG method for CH_4 flux estimates. The gradient method captured both the seasonal and diurnal CO_2 flux variability as the EC technique and the magnitudes agree well during the day, but during the night FG CO_2 flux was consistently lower throughout the experiment. Considering the differences in techniques, the results still agree quite well, which suggests that CH_4 fluxes can be trusted. Especially since CH_4 flux is most important during the warmer months, when the methods showed grater agreement compared to e.g. early spring. Nighttime data was frequently removed due to underdeveloped atmospheric turbulence. However, loss of nighttime data is not as big of an issue for CH_4 flux due to similar magnitudes throughout the diurnal cycle. Most of the time there was enough data to calculate daily averages despite nighttime loss. More complex gap filling methods can be used by utilizing dependency on e.g. temperature, water table depth and substrate availability, but for the purpose of this study the few gaps could be linearly interpolated. In addition to the promising CO_2 results, the CH_4 flux themselves exhibited similar dependencies on e.g. temperature and water table depth as found by other studies at similar sites. Finally, the cumulative CH_4 sums agree with findings from similar sites using other recognized measurement techniques.

Acknowledgements

I would like to thank my supervisors, Magnus Lund and Patrik Vestin. Magnus, thank you for introducing me to the field assistant job at Fäjemyr that led me into the topic of the project. And thank you for providing the data used throughout the study. Patrik, thank you for guiding me through the numerous rows of MATLAB-code and for always providing quick and helpful feedback. Finally, I would like to thank my friends and family for always believing in me and supporting me throughout the process.

6. References

Baldocchi, D. D. 2003. Assessing the eddy covariance technique for evaluating carbon dioxide exchange rates of ecosystems: past, present and future. Global Change Biology, 9: 479- 492.

Bellisario, L. M., Bubier, J. L., Moore, T. R. & Chanton, J. P. 1999. Controls on CH4 emissions from a northern peatland. Global Biogeochemical Cycles, 13, 81-91.

Burba, G., and D. Anderson. 2012. Brief Practical Guide to Eddy Covariance Flux Measurements: Principles and Workflow Examples for Scientific and Industrial Applications. LI-COR Biosciences, Version 1.0.1.

Businger, J. A., Wyngaard, J. C., Izumi, Y. & Bradley, E. F., 1971: Flux-profile relationships in the atmospheric surface layer. J. Atmos. Sci., 28, 181-189.

Christensen, T. R., Ekberg, A., Ström, L., Mastepanov, M., Panikov, N., Öquist, M., Svensson, B. H., Nykänen, H., Martikainen, P. J. & Oskarsson, H. 2003. Factors controlling large scale variations in methane emissions from wetlands. Geophysical Research Letters, 30, 1414.

Dengel, S., D. Zona, T. Sachs, M. Aurela, M. Jammet, F. J. W. Parmentier, W. Oechel, and T. Vesala (2013), Testing the applicability of neural networks as a gapfilling method using CH4 flux data from high latitude wetlands, Biogeosciences, 10(12), 8185–8200, doi:10.5194/bg-10-8185-2013.

Denmead, O. T. 2008. Approaches to measuring fluxes of methane and nitrous oxide between landscapes and the atmosphere. Plant Soil. 309, 5 24.

Dyer, A. J., 1974: A review of the flux profile relations. Boundary-Layer Meteorol., 1, 363-372.

Eniro, 2016, Aerial photograph, available December 2016: http://kartor.eniro.se/?c=56.2695,13.5490&z=15&l=aerial&g=56.2654,13.5535&q=%22r%C3%B6ke%22;yp

Foken, T. et al. (2004). Post-field data quality control. Handbook of Micrometeorology: A Guide for Surface Flux Measurements. X. Lee. Dordrecht, Kluwer: 81-108 in print.

Foken, T. 2008. Micrometeorology. Berlin Heidelberg: Springer- Verlag, pp. 179 222.

Foken, T., Aubinet, M., Leuning, J. 2012. "The Eddy Covariance Method". *Eddy Covariance: A Practical Guide To Measurement And Data Analysis*. Aubinet M, Vesala T and Papale D. 1st ed. Dordrecht, Heidelberg, London, New York: Springer, 2012.

Fratini, G., Ibrom, A., Burba, G. G., Arriga, N., and Pa- pale, D.: Relative humidity effects on water vapour fluxes measured with closed-path eddy-covariance systems with short sampling lines, Agric. For. Meterol., 165, 53–63, doi:10.1016/j.agrformet.2012.05.018, 2012.

Frolking, S., Roulet, N., and Fuglestvedt, J.: How northern peat- lands influence the earth's radiative budget: Sustained methane emission versus sustained carbon sequestration, J. Geophys. Res.-Bio., 111, G01008, doi:10.1029/2005JG000091, 2006.

Google Maps, 2016, available December 2016: https://www.google.se/maps/@56.2652877,13.5536277,1008m/data=!3m1!1e3

Gorham E (1991) Northern peatlands – role in the carbon-cycle and probable responses to climatic warming. Ecological Appli- cations, 1, 182–195.

Hargreaves, K.J., Fowler, D., Pitcairn, C.E.R., Aurela, M., 2001. Annual methane emission from Finnish mires estimated from eddy covariance campaign measurements. Theor. Appl. Climatol. 70, 203–213, http://dx.doi.org/10.1007/s007040170015.

Horst, T., and J. Weil, 1994. How far is far enough? The fetch requirement for micrometeorological measurement of surface fluxes. Journal or Atmospheric and Oceanic Technology, 11: 1018-1025

Högström (1988) Non-dimensional wind and temperature profiles in the atmospheric surface layer: a re-evaluation. Boundary-Layer Meteorology, 42, 55–78.

IPCC. 2013. Working group I contribution to the IPCC fifth assessment report, Climate change 2013: The physical science basis. Final draft underlying scientific-technical assessment. Intergovernmental panel on climate change.

Kaimal J C, Finnigan J J, 1994. Atmospheric boundary layer flows: their structure and measure- ment. Oxford: Oxford University Press.

Kim, J., Verma, S.B., Billesbach, D.P., and Clement, R.J., 1998b: Diel variation in methane emission from a midlatitude prairie wetland: Significance of convective throughflow in Phraghmites australis. J. Geophys. Res., 103, 28029-28039.

Kormann, R., Müller, H., and Werle, P., 2001: Eddy flux measurements of methane over the fen "Murnauer Moos", 11°11'E, 47°39'N, using a fast tunable diode laser spectrometer. Atmos. Environ., 35, 2533-2544.

Laine, A., Kiely, G., Byrne, K. A. & Wilson, D. 2007. Methane flux dynamics in an Irish lowland blanket bog. Plant and Soil, 299, 181-193.

Lafleur PM, Roulet NT, Bubier JL et al. (2003) Interannual variability in the peatland-atmosphere carbon dioxide ex- change at an ombrotrophic bog. Global Biogeochemical Cycles, 17, 1036, doi: 10.1029/2002GB001983.

Lai, D. Y. F. 2009. Methane dynamics in northern peatlands: A review. Pedosphere. 19(4): 409–421.

Laubach J., Barthel M., Fraser A. et al. (2016) Combining two complementary micrometeorological methods to measure CH_4 and N_2O fluxes over pasture. Biogeosciences, 13, 1309-1327, doi:10.5194/bg-13-1309-2016.

Laurila, T., Aurela, M., Tuovinen, J-P. 2012. "Eddy Covariance Measurements Over Wetlands". *Eddy Covariance: A Practical Guide To Measurement And Data Analysis*. Aubinet M, Vesala T and Papale D. 1st ed. Dordrecht, Heidelberg, London, New York: Springer, 2012. 354.

Leclerc MY, Thurtell GW (1990) Footprint prediction of scalar fluxes using a Markovian analysis. Boundary-Layer Meteorol 52:247–258

LI-7200. 2009. LI-7200 CO2/H2O Analyzer Instruction Manual. www.licor.com Publication No. 984-10564.

LI-COR, Inc. 2016. EddyPro® version 6.2 Help and User's Guide. LI-COR, Inc. Lincoln, NE.

Limpens, J., Berendse, F., Blodau, C., Canadell, J., Freeman, C., Holden, J., Roulet, N., Rydin, H., Schaepman-Strub, G., 2008. Peatlands and the carbon cycle: from local processes to global implications—a synthesis. Biogeosciences 5, 1475–1491, http://dx.doi.org/10.5194/bg-5-1475-2008.

Lund, M., Lindroth, A., Christensen, T.R., Strom, L., 2007. Annual CO_2 balance of a temperate bog. Tellus Ser. B 59, 804–811, http://dx.doi.org/ 10.1111/j.1600-0889.2007.00303.x.

Lund, M. 2009. Peatlands at a Threshold - Greenhouse Gas Dynamics in a Changing Climate, Lund, Sweden, Lund University.

Lund, M., Christensen, T.R., Lindroth, A., Schubert, P., 2012. Effects of drought conditions on the carbon dioxide dynamics in a temperate peatland. Environ. Res. Lett. 7, 045704.

MATLAB (2015). Version R2015b. The MathWorks Inc., Natick, MA.

Mauder, M. & Foken, T. (2004) Quality control of eddy covariance measurements (C: 0,1,2). CARBOEUROPE-IP

Mitsch WJ, Gosselink JG, Anderson CJ, Zhang L (2009) Wetland ecosystems. Wiley, Hoboken, 295 pp

Moncrieff, J.B., Massheder, J.M., deBruin, H., Elbers, J., Friborg, T., Heusinkveld, B., Kabat, P., Scott, S., Soegaard, H., Verhoef, A., 1997. A system to measure surface fluxes of momentum, sensible heat, water vapour and carbon dioxide. J. Hydrol. 189, 589–611, http://dx.doi.org/10.1016/S0022-1694(96)03194-0.

Rinne J, Riutta T, Pihlatie M, Aurela M, Haapanala S, Tuovinen J-P, Tuittila E-S, Vesala T (2007) Annual cycle of methane emission from a boreal fen measured by the eddy covariance technique. Tellus B 9:449–457

Reichstein, M., E. Falge, D. Baldocchi, D. Papale, M. Aubinet, P. Berbigier, C. Bernhofer, N. Buchmann, et al. 2005. On the separation of net ecosystem exchange into assimilation and ecosystem respiration: review and improved algorithm. Global Change Biology, 11: 1424-1439. DOI: 10.1111/j.1365-2486.2005.001002.x

Schmid HP, Grimmond CSB, Cropley F, Offerle B, Su H-B (2000) Measurements of CO2 and energy fluxes over a mixed hardwood forest in the mid-western United States. Agric For Meteorol 103:357–374

Sundqvist, E., Mölder, M., Crill, P., Kljun, N., Lindroth, A. (2015) Methane exchange in a boreal forest estimated by gradient method. Tellus B 2015, 67, 26688, http://dx.doi.org/10.3402/tellusb.v67.26688

Suyker, A.E., Verma, S.B., Clement, R.J., and Billesbach, D.P., 1996: Methane flux in a boreal fen: Season-long measurement by eddy correlation. J. Geophys. Res., 101, 28637- 28647.

Tagesson, T., Mölder, M., Mastepanov, M., et al. (2012) Land-atmosphere exchange of methane from soil thawing to soil freezing in a high-Arctic wet tundra ecosystem. Global Change Biology (2012) 18, 1928–1940, doi: 10.1111/j.1365-2486.2012.02647.x

Tagesson, T. Turbulent transport in the atmospheric surface layer, SKB report TR-12-05

Vickers, D. and L. Mahrt, 1997. Quality control and flux sampling problems for tower and aircraft data. Journal of Atmospheric and Oceanic Technology, 14: 512-526

Wille C, Kutzbach L, Sachs T, Wagner D, Pfeiffer E-M (2008) Methane emission from Siberian arctic polygonal tundra: eddy covariance measurements and modeling. Global Change Biology, 14, 1395–1408.

Institutionen för naturgeografi och ekosystemvetenskap, Lunds Universitet.
Student examensarbete (Seminarieuppsatser). Uppsatserna finns tillgängliga på institutionens geobibliotek, Sölvegatan 12, 223 62 LUND. Serien startade 1985. Hela listan och själva uppsatserna är även tillgängliga på LUP student papers (https://lup.lub.lu.se/student-papers/search/) och via Geobiblioteket (www.geobib.lu.se)
The student thesis reports are available at the Geo-Library, Department of Physical Geography and Ecosystem Science, University of Lund, Sölvegatan 12, S-223 62 Lund, Sweden. Report series started 1985. The complete list and electronic versions are also electronic available at the LUP student papers (https://lup.lub.lu.se/student-papers/search/) and through the Geo-library (www.geobib.lu.se)

372 Andreas Dahlbom (2016) The impact of permafrost degradation on methane fluxes - a field study in Abisko
373 Hanna Modin (2016) Higher temperatures increase nutrient availability in the High Arctic, causing elevated competitive pressure and a decline in *Papaver radicatum*
374 Elsa Lindevall (2016) Assessment of the relationship between the Photochemical Reflectance Index and Light Use Efficiency: A study of its seasonal and diurnal variation in a sub-arctic birch forest, Abisko, Sweden
375 Henrik Hagelin and Matthieu Cluzel (2016) Applying FARSITE and Prometheus on the Västmanland Fire, Sweden (2014): Fire Growth Simulation as a Measure Against Forest Fire Spread – A Model Suitability Study –
376 Pontus Cederholm (2016) Californian Drought: The Processes and Factors Controlling the 2011-2016 Drought and Winter Precipitation in California
377 Johannes Loer (2016) Modelling nitrogen balance in two Southern Swedish spruce plantations
378 Hanna Angel (2016) Water and carbon footprints of mining and producing Cu, Mg and Zn: A comparative study of primary and secondary sources
379 Gusten Brodin (2016) Organic farming's role in adaptation to and mitigation of climate change - an overview of ecological resilience and a model case study
380 Veränika Trollblad (2016) Odling av *Cucumis Sativus* L. med aska från träd som näringstillägg i ett urinbaserat hydroponiskt system
381 Susanne De Bourg (2016) Tillväxteffekter för andra generationens granskog efter tidigare genomförd kalkning
382 Katarina Crafoord (2016) Placering av energiskog i Sverige - en GIS analys
383 Simon Nåfält (2016) Assessing avalanche risk by terrain analysis An experimental GIS-approach to The Avalanche Terrain Exposure Scale (ATES)
384 Vide Hellgren (2016) Asteroid Mining - A Review of Methods and Aspects
385 Tina Truedsson (2016) Hur påverkar snömängd och vindförhållande vattentrycksmätningar vintertid i en sjö på västra Grönland?
386 Chloe Näslund (2016) Prompt Pediatric Care Pediatric patients' estimated travel times to surgically-equipped hospitals in Sweden's Scania County
387 Yufei Wei (2016) Developing a web-based system to visualize vegetation trends by a nonlinear regression algorithm
388 Greta Wistrand (2016) Investigating the potential of object-based image analysis to identify tree avenues in high resolution aerial imagery and lidar data

389 Jessica Ahlgren (2016) Development of a Web Mapping Application for grazing resource information in Kordofan, Sudan, by downloading MODIS data automatically via Python
390 Hanna Axén (2016) Methane flux measurements with low-cost solid state sensors in Kobbefjord, West Greenland
391 Ludvig Forslund (2016) Development of methods for flood analysis and response in a Web-GIS for disaster management
392 Shuzhi Dong (2016) Comparisons between different multi-criteria decision analysis techniques for disease susceptibility mapping
393 Thirze Hermans (2016) Modelling grain surplus/deficit in Cameroon for 2030
394 Stefanos Georganos (2016) Exploring the spatial relationship between NDVI and rainfall in the semi-arid Sahel using geographically weighted regression
395 Julia Kelly (2016) Physiological responses to drought in healthy and stressed trees: a comparison of four species in Oregon, USA
396 Antonín Kusbach (2016) Analysis of Arctic peak-season carbon flux estimations based on four MODIS vegetation products
397 Luana Andreea Simion (2016) Conservation assessments of Văcărești urban wetland in Bucharest (Romania): Land cover and climate changes from 2000 to 2015
398 Elsa Nordén (2016) Comparison between three landscape analysis tools to aid conservation efforts
399 Tudor Buhalău (2016) Detecting clear-cut deforestation using Landsat data: A time series analysis of remote sensing data in Covasna County, Romania between 2005 and 2015
400 Sofia Sjögren (2016) Effective methods for prediction and visualization of contaminated soil volumes in 3D with GIS
401 Jayan Wijesingha (2016) Geometric quality assessment of multi-rotor unmanned aerial vehicle-borne remote sensing products for precision agriculture
402 Jenny Ahlstrand (2016) Effects of altered precipitation regimes on bryophyte carbon dynamics in a Peruvian tropical montane cloud forest
403 Peter Markus (2016) Design and development of a prototype mobile geographical information system for real-time collection and storage of traffic accident data
404 Christos Bountzouklis (2016) Monitoring of Santorini (Greece) volcano during post-unrest period (2014-2016) with interferometric time series of Sentinel-1A
405 Gea Hallen (2016) Porous asphalt as a method for reducing urban storm water runoff in Lund, Sweden
406 Marcus Rudolf (2016) Spatiotemporal reconstructions of black carbon, organic matter and heavy metals in coastal records of south-west Sweden
407 Sophie Rudbäck (2016) The spatial growth pattern and directional properties of *Dryas octopetala* on Spitsbergen, Svalbard
408 Julia Schütt (2017) Assessment of forcing mechanisms on net community production and dissolved inorganic carbon dynamics in the Southern Ocean using glider data
409 Abdalla Eltayeb A. Mohamed (2016) Mapping tree canopy cover in the semi-arid Sahel using satellite remote sensing and Google Earth imagery
410 Ying Zhou (2016) The link between secondary organic aerosol and monoterpenes at a boreal forest site

411 Matthew Corney (2016) Preparation and analysis of crowdsourced GPS bicycling data: a study of Skåne, Sweden
412 Louise Hannon Bradshaw (2017) Sweden, forests & wind storms: Developing a model to predict storm damage to forests in Kronoberg county
413 Joel D. White (2017) Shifts within the carbon cycle in response to the absence of keystone herbivore Ovibos moschatus in a high arctic mire
414 Kristofer Karlsson (2017) Greenhouse gas flux at a temperate peatland: a comparison of the eddy covariance method and the flux-gradient method